The Ultraviolet Radiosensitivity of *Oedogonium cardiacum* Cells at Various Stages of the Cell Cycle

by

Kirsten Elisabeth Parker, B.A.

A Thesis Submitted to the Faculty of Graduate Studies in Partial Fulfilment of the Requirements for the Degree Master of Science

McMaster University

May, 1969

The Ultraviolet Radiosensitivity of

Oedogonium cardiacum

MASTER OF SCIENCE (1969) McMASTER UNIVERSITY
(Biology) Hamilton, Ontario.

TITLE: The Ultraviolet Radiosensitivity of *Oedogonium cardiacum* Cells at Various Stages of the Cell Cycle

AUTHOR: Kirsten Elisabeth Parker, B.A. (Hons.) (University of New Brunswick)

SUPERVISORS: Drs. R.J. Horsley and S. Mak

NUMBER OF PAGES: ix, 111

SCOPE AND CONTENTS:

The ultraviolet radiosensitivity of synchronously growing *O. cardiacum*, was measured during the first generation cycle and compared to the radiosensitivity to ionizing radiation. Both radiosensitivity patterns were approximately the same in shape exhibiting a maximum resistance in S and a minimum in G_2. Following x-radiation Do and n values varied with age by a factor of 7 and 40 respectively. In contrast following UV radiation Do varied by a factor of 2.5 and n remained essentially constant. A seasonal variation in the magnitude of the UV radiosensitivity was observed and is attributed to seasonal differences in UV cytoplasmic absorption. A complex survival curve was obtained at all cell ages and dose levels. An explanation for the shape of the complex curve involving cytoplasmic UV attenuation and the additive effects of UV-induced cytoplasmic damage at high dose levels is favoured. Preliminary investigations showed that photoreactivation does occur.

ACKNOWLEDGEMENTS

I wish to express my sincere gratitude to Drs. R.J. Horsley and S. Mak under whose supervision this work was carried out.

Also, I wish to thank the members of the Department of Physics and Radiobiology at the Ontario Cancer Treatment and Research Foundation, Hamilton Clinic who in numerous ways have assisted me in this work. To Mrs. Donna Johnston who typed this thesis, I am also indebted.

The financial support of the National Research Council of Canada is greatly appreciated.

Dept. of Biology
McMaster University
May, 1969

PREFACE

This thesis describes work carried out at the Ontario Cancer Treatment and Research Foundation, Hamilton Clinic, in association with the Department of Biology, McMaster University, from September 1967 to March 1969.

The aim of this investigation was to determine the radiosensitivity, as measured by loss of proliferative capacity, of Oedogonium cardiacum irradiated by UV radiation at different ages in the first generation cycle. In the Introduction an attempt has been made to review the salient features of relevant UV radiation research particularly of the past fifteen years in order to provide a background to the topic of the investigation. In Chapters I and II respectively the Materials and Methods and Results of the investigation are presented. In Chapter III, the Discussion, the results are compared to those of other workers studying the effects of UV radiation on synchronized cultures of both plant and mammalian cells.

TABLE OF CONTENTS

LIST OF FIGURES

LIST OF TABLES

INTRODUCTION

The effects of ultraviolet (UV) radiation on both the molecular and cellular level have been studied in many biological systems, including higher and lower organisms. In addition, the effects of UV on isolated biological components, in particular the nucleic acids and their constituents, have been the subject of numerous investigations. As a result of these investigations it has been demonstrated that a large proportion of UV-induced biological damage arises from photochemical changes in the nucleic acids. It has also been shown that many biological systems are capable of reducing changes. This Chapter will review some of the salient features of recent UV radiation research, in particular that concerned with the identification of molecular lesions induced by UV absorption, the repair of these lesions, and the effects of these lesions biologically. For a more comprehensive review and historical survey of literature in this field, reviews by Setlow (1), Giese (2), Jagger (3), Hollaender (4) and Bowen (5) are available.

A. UV-Induced Molecular Lesions

The hypothesis that the majority of the effects of UV radiation on living organisms can be ascribed to photochemical alterations in deoxyribonucleic acid (DNA) has been strongly supported by several investigations. When isolated DNA was exposed to monochromatic UV radiation it absorbed most strongly in the region of 2600Å, the same region found to produce the greatest effects on living organisms (6, 7, 8, 9). Since at 2600Å, the four bases comprising DNA, adenine, guanine, thymine and cytosine, were largely responsible for UV absorption (10), it is reasonable to assume that much of the deleterious action of UV arises from photochemical changes in these bases.

Many different UV-induced physical and chemical changes which have been observed in UV-irradiated DNA and its bases have been implicated as the mechanism by which UV produces biological damage (see review: 1). These photochemical changes include, purine and pyrimidine dimers and hydrates (11, 12, 18), DNA chain breaks and cross links (1), and DNA-protein cross links (13). At the present time, the dimerization of pyrimidines, in particular thymine, is considered the principal reaction for the alteration of the biological activity of DNA. This hypothesis is supported by the results of several investigators. Setlow and Setlow (14) found that at high UV doses about 50% of the biological inactivation of the transforming activity of Hemophilus influenzae was due to thymine dimer formation. Trosko (15)

has shown that thymine dimers can be induced in mammalian chromosomal DNA by UV, and that the number of dimers induced increased linearly with dose. Wulff (16) found that the UV inactivation of T4V bacteriophage led to the formation of 4.8 thymine dimers per lethal hit.

The remainder of the UV induced lesions mentioned previously are not believed to contribute significantly to the biological effects of UV except at extremely high doses or in the case of UV resistant cells such as Micrococcus radiodurans (17). However, thymine dimer formation is not sufficient to explain all the observed inactivations by UV (7). UV radiation is also absorbed by the proteins, ribonucleic acid (RNA), and other nuclear and cytoplasmic components which play a role in the cell metabolism, and therefore it presumably induces lesions in these components.

Comparatively little is known about the photochemistry of RNA (see review: 5). Cytosine and uracil hydrates and dimers have been observed in UV-irradiated polynucleotides (18); however, their role in biological inactivation "in vivo" is poorly understood. Swenson et al (19) have shown that over 95% of the UV-induced absorbance changes in poly uridylic acid (poly-U) were attributable to the sum of dimer formation and photohydration of uracil residues, their relative amounts depending on dose and wavelength. Grossman (20) has shown

that the coding properties of UV-irradiated poly-U were altered when it was used as a messenger in an "in vitro" polypeptide synthesizing system; however, the nature of these alterations was not understood.

The effects of UV on proteins "in vivo" is also poorly understood. Alexander and Moroson (13) have shown that UV irradiation of Eschericha coli 15 T⁻ made the DNA susceptible to cross-linking with proteins. The amounts of DNA that could be extracted from the UV-irradiated cells decreased with increasing UV doses. Smith (21) has shown that the extent of cross-linking was dependent on cell age, that is, the position in the cell cycle occupied by the cell at the time of irradiation.

Although the aromatic amino acids of proteins are good UV absorbers "in vitro", they are believed to be relatively unimportant in protein inactivation "in vivo" (see review: 22). Cystine is believed to be the most important amino acid target in protein inactivation "in vivo"; however, the biological effects of this inactivation are unknown.

B. Repair of UV-Induced Damage

Mechanisms for the repair of UV-induced damage exist in many biological systems. This can be concluded from the observation that many cells are able to markedly decrease the potential biological effects of UV-induced damage (23, 24, 25, 26). Two mechanisms for the enzymatic repair of UV-induced damage have been proposed. Both mechanisms, photoreactivation (27) and dark repair (28) are dependent on post-irradiation treatment. Although each mechanism has been described with respect to bacteria, the same principals are believed to be applicable to the higher organisms.

Rupert has described the mechanism of photo-reactivation in a series of reviews (29, 30, 31, 32). It involves a light-activated enzymatic reaction by which pyrimidine dimers are monomerized. He was able to extract an active factor from the blue green alga Plectonema boryanum (32) and also from baker's yeast (31) which when incubated in white light with UV-irradiated transforming DNA, extracted from Hemophilus influenzae, produced a recovery of transforming activity. This recovery was absent when incubation occurred in the dark, or in the absence of the active factor. The kinetics of the reaction between the active factor and the transforming DNA fit an enzyme-substrate scheme (27). The active factor or enzyme formed a complex with only irradiated DNA. During illumination

the complex separated, and the ability of the DNA to bind the enzyme was lost. Since thymine dimers were eliminated in the reaction, as was shown by acid hydrolysis of the entire mixture of yeast extract and DNA (33), the dimers were believed to be the substrate for the enzyme. Other substrates, in additon to thymine, cytosine and uracil dimers can compete for the enzyme, resulting in a decreased rate of reactivation of the transforming DNA. Setlow found that with maximum photoreactivation of UV-irradiated transforming DNA, 90% of the biological damage could be eliminated and all the thymine dimers removed (27).

Photoreversal of UV-induced damage affecting nuclear events such as mutation induction, mitotic rate, and DNA synthesis has been observed in plants (26), protozoa (37), bacteria (38), fungi (39) and viruses (40). It has not been reported in the literature for UV-irradiated cultured mammalian cells.

All known examples of cellular photoreactivation have been accounted for on the basis of reactivation of either RNA or DNA (see review: 3). Marcenko (34) and von Borstel and Wolff (35) investigated the localization of the photoreactivation phenomenon within the cell. Marcenko found that photoreactivation of the lesions responsible for loss of reproductive integrity in the alga Netrium digitus was associated primarily with the region of the cell containing the nucleus. This agrees with the model of photo-enzymatic repair by Rupert in which the photoreactivating

light had to be absorbed by the complex of irradiated DNA and photoreactivating enzyme. Von Borstel and Wolff observed that certain expressions of nuclear damage in Habrobracon juglandis eggs could be partly reversed by exposing the nucleus to photoreactivating light; however, photoreactivation could not be detected after illuminating the injured cytoplasm. Since other investigators (17, 48) have shown evidence for photoreactivable sites in the cytoplasm which may or may not be associated with RNA or DNA, the possibility remains that important sites for absorption of photoreactivating light may be outside the nucleus.

The other principal mechanism for repair, namely dark repair or the enzymic excision of pyrimidine dimers from the damaged DNA, has been observed in bacteria (41), yeast (42), virus (43), mammalian (25) and plant cells (26). The biochemical pathway for this type of repair is believed to have steps in common with those of genetic recombination by breakage reunion (44). Szybalski (45) has proposed a scheme for the enzymatic events which result in this repair process. In his scheme four enzymes, A, B, C, and D are involved. Enzyme A recognizes the UV-induced damage and severs the adjoining phosphate-ester bond of the nucleotide. Enzyme B, an exonuclease, excises the damaged nucleotide together with a few adjacent ones. Enzyme C, a DNA polymerase, synthesizes the new nucleotides using the complementary DNA strand as a template, and

enzyme D, a ligase joins the phosphate-ester bond between the newly synthesized nucleotide and the remainder of the DNA chain.

There are several lines of evidence for support of this excision mechanism. Howard-Flanders et al (28) have shown that thymine dimers formed in the DNA of UV-irradiated E. coli K12 were gradually released and could be extracted by cold acid if the bacteria was incubated in nutrient medium after UV irradiation. The excision of the thymine dimers appeared to be part of the repair process, as UV-irradiated E. coli K12 mutants that were unable to excise the dimers were also more sensitive to UV radiation. An unscheduled DNA synthesis has been observed following the UV irradiation of E. coli (28), Chinese hamster cells (46), and HeLa cells (47). It has been suggested that this unscheduled DNA synthesis could be explained by the dark repair mechanism since it was not semi-conservative, was enhanced by BUdR addition and showed little variation in tritiated thymine uptake (28). Setlow (28) has shown that when UV-irradiated E. coli was grown with 5-bromouracil (BU), the BU appeared to be incorporated into the DNA at a number of sites along the molecule. It is suggested that these sites may be the repair zones described above and represent the region where the nucleotides have been inserted.

C. Expressions of UV-Induced Biological Damage

The cellular and sub-cellular expressions of UV-induced damage are numerous and varied. It is well established that UV inactivates cells, viruses and biologically active DNA's. In addition it induces mutation, causes chromosomal aberration, inhibits DNA synthesis and induces other lethal and non-lethal expressions of radiation damage.

UV-induced gene mutations and chromosome aberrations in both higher and lower organisms have been reported by several workers (see review: 15). The mechanism of UV-induced mutation is not understood. "In vitro" studies of DNA have shown that pyrimidine dimers cause measurable base changes in DNA; however, none of these studies have equated photochemical changes with mutation (1). Kimball has shown that some premutational lesions were susceptible to repair and that there existed a terminal event beyond which further modification could not occur (49). Howard and Tessman found that UV-induced mutations in bacteriophage S13 resulted from a base deletion, addition or transition (50). Hass and Doudney have shown that RNA and protein synthesis were required for mutation induction in E. coli (51). When chloramphenicol, an inhibitor of protein synthesis, was added to the culture medium of UV-irradiated E. coli, only those cells that had already synthesized their RNA and protein prior to the addition acquired mutants. Other investigators have shown

that mutation frequency can be altered by post-irradiation treatments with drugs and other agents (see review: 1).

The use of UV to induce or isolate mutants in algae has been reported by several investigators. Kumar exposed the blue green alga Anacystis nidulans to UV radiation during successive subcultures and found that the strain obtained was more resistant to UV than the original stock culture (52). Lewin isolated mutants in the unicellular green alga Chlamydomonas moewussi, that could be recognized by features of their cell content, form, motility or mode of division (58). In addition, Bendix and Allen (54) and Anikeeva (55) have isolated UV resistant mutants from different species of UV-irradiated Chlorella.

Chromosomal damage in cells irradiated with UV in various phases of the cell cycle has been reported by Humphrey et al (56). Cells synthesizing DNA at the time of irradiation suffered about ten times the chromosomal damage of cells in G_1 and G_2 phases[(a)]. The greatest fraction of damage was elicited as chromatid exchanges and breaks. Faberge treated Zea mays endosperm pollen containing four dominant linked markers with UV radiation and

(a) The cell cycle of plant (58) and mammalian (59) cells has been divided into four stages which are related to the stage at which DNA is synthesized. These stages are called S, the interval during which DNA is synthesized; G_2, the interval following DNA synthesis and before mitosis; mitosis M, the interval during which nuclear division takes place; and G_1, the interval following mitosis and before the onset of DNA synthesis.

obtained mosaic patterns with several kinds of chromosomal aberrations. These he identified as dicentrics, rings, translocations, inversions or bridges (57).

The rate of progression of cells through the generation cycle is altered by UV exposure. Domon and Rauth (60), and Djordjevic and Tolmach (47) have shown that low exposures of UV irradiation could depress DNA synthesis and delay the progression of cells about the cell cycle. Cells irradiated in G_1 or G_2 exhibited no delay in their progression to S or M respectively. Deering observed that nuclear division delay in Blastocladiella emersonii was also dependent on cell age at irradiation (61). Damage produced prior to DNA replication effectively blocked nuclear division while damage induced after DNA replication had little effect on the separation of the daughter nuclei.

The rate of DNA synthesis following UV radiation has been investigated in several cultured mammalian cells by Cleaver (62, 63, 64). He found that depression in the rate of DNA synthesis due to UV irradiation varied with the position of the cell in the S stage at the time of irradiation. At doses above 240 ergs/mm^2 a complete and irreversible cessation of DNA synthesis was reported, with lysis of most of the cells occurring within 10 to 20 hours. At lower doses, recovery of DNA synthesis occurred after longer periods of time.

A complete loss of cellular metabolic activity prior to completion of the first post-irradiation mitosis has

been reported in mammalian, plant and yeast cells (65, 47, 67, 68, 61). The biochemical mechanisms responsible for this mode of cell death, referred to as interphase death, have not yet been elucidated. Scaife and Brohee (65) observed that cultured human kidney epithelial cells were most susceptible to interphase death if irradiated during S and M, and least sensitive during G_1 and G_2. Swann (68) found that at high UV doses, increased lethality in the fission yeast Schizosaccharomyces pombe was mainly made up of cells that die without dividing. He postulated that this interphase death was a consequence of nongenetic damage superimposed on genetic damage.

In addition to the manifestations of UV-induced damage previously mentioned, UV radiation can also alter the properties of cell and nuclear membranes (2), delay the synthesis of certain substances by cells (69), inactivate enzyme formation (6), cause embryo abortion (72) and induce more specific responses in cells such as deflagellation (71).

The biological expression of UV-induced damage is dependent not only on the UV dose but in many cases is also dependent on cell age at the time of irradiation. This has been recognized in terms of mutation, chromosome damage and lethality as mentioned above.

Studies of UV stage sensitivity in terms of lethality have been done on bacteria (73), yeast (68, 74), fungi (66), mammalian (47, 67, 65, 46, 75) and plant (26, 61)

cells. Variations in radiosensitivity patterns observed in mammalian cells, namely mouse L cells, Detroit 98/AG cells, Chinese hamster V79 cells and human epithelial kidney cells were correlated with the G_1, S, G_2, and M stages. However, in the relatively few cultured plant cells investigated to date, namely C. reinhardii and B. emersonii, this was not possible. In both plants, no method has been found to specifically label the DNA of the organism. This was due largely to the complexity of the normal division cycle in Chlamydomonas and to the lack of incorporation of specific DNA precursors in Blastocladiella. The small amount of DNA relative to RNA in Blastocladiella also complicated chemical and isotopic assays.

The work to be described represents part of the general radiobiological studies which have been undertaken in this laboratory using O. cardiacum. Investigations concerning the radiosensitivity of O. cardiacum to ionizing radiation have previously been made during the first generation cycle in terms of changes in the proliferative capacity (76-79). Other expressions of lethal radiation damage (80-82) such as giant cell formation have also been investigated. In this treatise, the UV radiosensitivity of O. cardiacum cells at various stages of the cell cycle will be described. The response pattern observed will be compared to the variations in UV radiosensitivity with cell age for other organisms which have been reported in the literature. In addition, the response pattern will be com-

pared to the previously reported pattern for the radiosensitivity of O. cardiacum to ionizing radiation (79).

CHAPTER I

MATERIALS AND METHODS

A. Cell Line

The morphology, growth habit and life cycle of O. cardiacum have been described in detail by several workers (83, 84, 85); however, a brief description of the salient features follow.

O. cardiacum is a fresh water green alga which consists of uninucleate cells joined end to end to form unbranched filaments of indefinite length. Each cell is about 80 to 100 μ long and 30 μ wide, and contains a peripheral reticulate chloroplast with pyrenoids. The filaments have an apical-basal polarity and are attached to the substratum by a specially differentiated basal cell. Any cell is capable of mitosis, which is accompanied by the formation of an apical cap providing a persistent record of the number of cellular divisions in the filament.

Oedogonium is heterothallic and both asexual and sexual reproduction occur. In asexual reproduction, multiflagellate, phototropic zoospores formed singly in vegetative cells are released apically by a rupture in the

cell wall. Following a swimming period, which normally lasts for a short period of time, the zoospores come to rest with their anterior or flagella end down. The flagella disappear and the zoospore develops into a germling through elongation and formation of an attachment structure or holdfast. Forms which do not become attached to the substratum frequently die off or release their contents (86). Secondary spore formation from the one-celled germling can occur, rather than its development to a filament through cell division.

Sexual reproduction is of an advanced oogamous type. Each oogonium contains a single large oospore and each antheridium normally two sperms. The fertilized egg develops into a thick-walled diploid zygote which is liberated by decay of the oogonial wall. Following a resting period which may last for several months, the zygote undergoes mitosis, germinates and liberates four haploid zoospores which give rise to unisexual male and female plants.

B. Growth Conditions

Female haploid O. cardiacum cultures 3 to 5 months old were used in all the experimental investigations. The stock cultures were obtained from the Indiana State University Culture Collection of Algae and were routinely subcultured in the laboratory.

Cultures were maintained in 1:12 diphasic soil-water medium[b] in one quart jars fitted with tops through which a hole had been bored and plugged with cotton. Each jar was boiled for 2 separate 2 hour periods at 1 week interval and then innoculated with small portions of washed filaments after the supernatant had lost its turbidity.

Cultures were initially maintained at room temperature under a 12:12 hr diurnal light-dark cycle on an illuminated culture rack of light intensity 75 to 100 foot candles (ft-c). After one month, they were transferred to a north window for subsequent growth.

Cultures that were initiated from spores which had survived high doses of UV radiation were prepared by innoculating the glass jars with a single surviving filament. These cultures are referred to as UV-irradiated cultures throughout this treatise.

C. Zoosporogenesis and Spore Collection

Synchronous cell populations were obtained by inducing vegetative filaments to sporulate, and collecting the subsequent spores over a short time period. Using the procedure to be described, a population of cells, all at about the same point in the cell cycle (early G_1), was obtained.

Vegetative filaments were removed from the culture

(b) Dry powdered garden soil from Aldershot, Ontario was used.

jars, washed in distilled water and placed into a 500 ml Erlenmyer flask which contained 1:3 soil-water extract. (Refer to Appendix A for preparation of soil extract.) Each flask was covered with aluminum foil to exclude the light and plugged with a foam rubber stopper through which a glass "bubbler" tube (i.e., pasteur pipette) was inserted. The solution was bubbled with a mixture of 1% CO_2 and filtered air at a rate of 50 ml/min. Depending on the condition of the filaments, zoosporogenesis took place within 36 $\pm$ 6 hr.

To collect the spores, the solution was poured over glass microscope slides (7.5 cm x 2.5 cm) which lined the bottom of a perspex vessel. The sides and top of the vessel were darkened to allow light to enter only from the bottom. This vessel was placed on a surface illuminated with warm white fluorescent bulbs and the phototropic spores were collected at a light intensity of about 300 ft-c. After a collection period of 1 hr, which was normally sufficient to yield approximately 1000 spores of uniform age on each slide, the slides were rinsed in distilled water to remove unattached spores and debris, and then transferred to perspex culture vessels containing modified Machlis' Medium E. This medium will be referred to as growth medium throughout this treatise. (Refer to Appendix A for its preparation.) The samples were grown in the culture vessels in a temperature controlled bath at 22 $\pm$ 0.5°C which was illuminated from below by warm white fluorescent

lamps at a light intensity of about 300 ft-c.

At the end of the 5 day growing period, the samples were removed from the culture vessels, rinsed with distilled water and fixed for at least 15 min with 3:1 alcohol:acetic acid (Carnoy's Solution). They were examined as temporary mounts in 70% alcohol prepared by placing a glass cover over the fixed material. The cover, held in place by 2 rubber bands, protected and pressed the material. If the mounts were not to be examined immediately, they were stored in 70% ethanol at 4°C.

D. Measurement of Synchrony

To estimate the synchrony of each cell population collected, an index of synchrony as described by Zeuthen (87), namely the percent phasing, was used. Slides were examined at hourly intervals from 12 to 24 hr after the mid-point of the collection period and the number of cells which had divided at least once, as a function of fixation time was determined. In all experiments, a sporeling which showed signs of stretching of the cylinder of new cell wall material following karyokinesis was accepted as having divided.

E. Ultraviolet Source and Dosimetry

Two 15-watt germicidal low pressure mercury vapor lamps[c] emitting primarily 2537Å were used as the UV

(c) General Electric Co.
(d) Ultraviolet Products Inc., San Gabriel, California.

source. These were mounted parallel 47.6 cm above a designated target plane and connected to the output of a voltage stabilizer which maintained a constant voltage of 119 volts. The duration of the radiation period was controlled by a synchronous timer incorporated into the electrical system. The lamps were switched on approximately one hour prior to starting the radiations to stabilize their energy output. A photograph of the apparatus is shown in Fig. 1.

Since a relatively large area was required for irradiating the samples it was necessary to insure a uniform dose. Therefore, the distribution of the UV radiation on the target plane was determined using a UV sensitive photocell[(d)] and a galvanometer. The photocell was positioned at different areas on the target plane at the exposure distance, and the incident intensity read in arbitrary units from the meter. Each reading was expressed as a percentage of the maximum reading which was set equal to 100%, and iso-intensity curves plotted to determine the area in which the incident UV radiation varied within 5 percent.

Using the same photocell, the deterioration of the lamps as measured by the percentage of white light emitted was determined. The photocell was positioned on the target plane at the exposure distance, and the incident intensity recorded in the absence and presence of a perspex

FIG. 1

Ultraviolet radiation apparatus showing sensor cell in center of target plane. Instruments on top of apparatus are: UV intensity meter, synchronous timer, volt meter, galvanometer and voltage stabilizer.

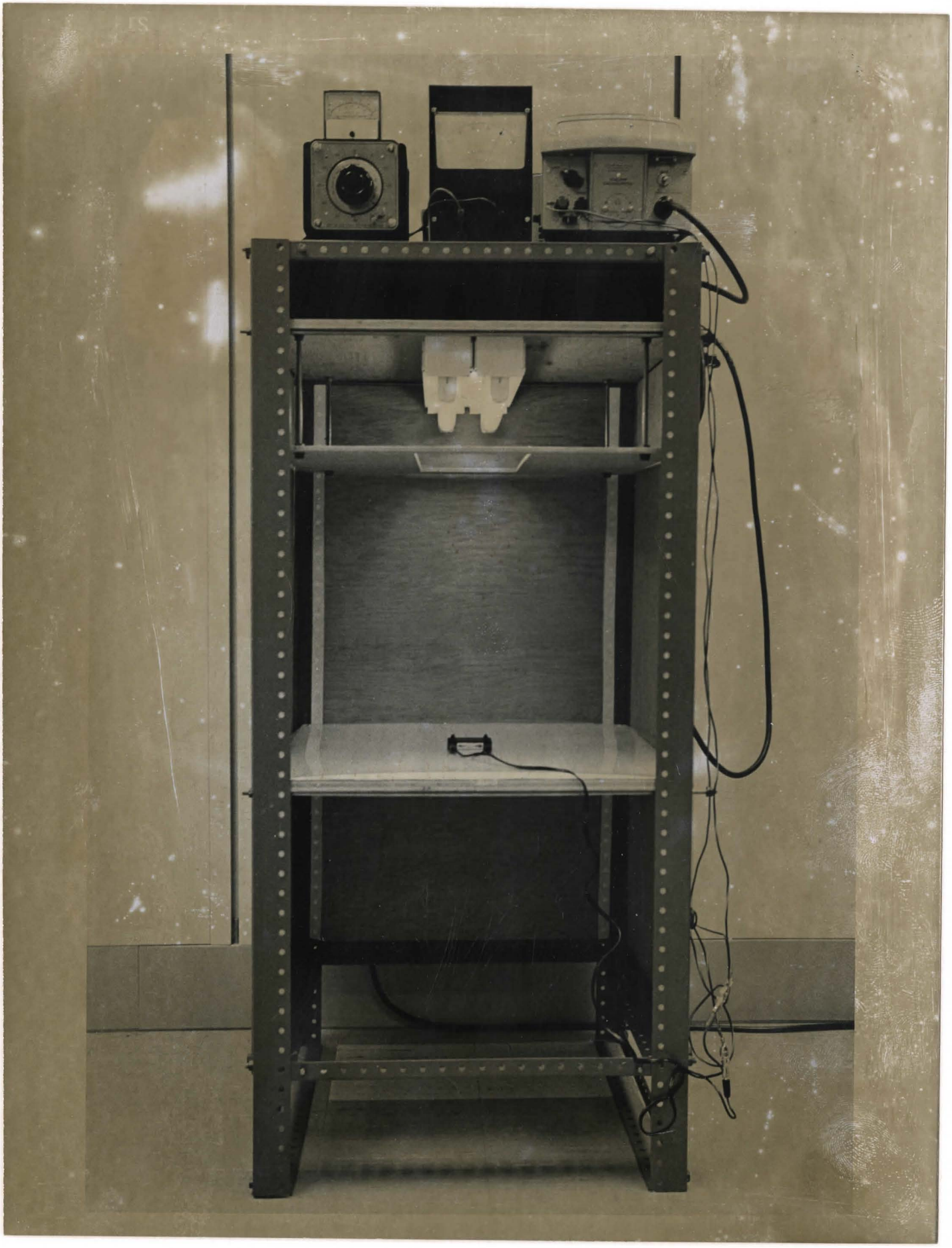

UV absorber. This value which ranged between 7.4 and 8.7% during the experimental period was considered in calibrating the apparatus.

The UV apparatus was calibrated with a UV intensity meter and sensor cell(d) calibrated by a standard traceable to the U.S. National Bureau of Standards and also with ϕx-174 bacteriophage(e), a biological dosimeter.

To measure the incident intensity with the calibrated meter, the sensor cell was placed in the center of the target plane and the intensity read in uW/cm^2 from the meter. The percentage white light emitted from the lamps was subtracted from the reading, to obtain the corrected UV intensity.

When ϕx-174 bacteriophage was used as a dosimeter, the phage was diluted in phosphate buffer saline (PBS) and exposed to the UV radiation in an open petri dish. Small aliquots were removed at intervals, diluted and plated for plaque forming ability (pfu) on E. coli C 3000(e) by the soft agar technique (92). After incubation for 3 to 6 hr at 37°C, the plaques were counted and survival curves constructed assuming a Do(f) of 85 $ergs/mm^2$ (67). The average dose incident on the

(e) Courtesy of Dr. A.M. Rauth, Dept. of Biophysics, Princess Margaret Hospital, Toronto, Ontario.
(f) The Do value represents the dose required to reduce survival by e^{-1} along the exponential portion of the survival curve obtained when log percent survival is plotted as a function of dose.

medium was calculated using the correction of Morowitz (90). (Refer to Appendix C for details of calibration procedure.)

In both procedures, the sensor cell and petri dish were positioned at the center of the target plane at an exposure distance of 71.0 cm.

F. Irradiation Procedure

The samples were exposed to the UV radiation in an open perspex vessel (13 cm x 19 cm x 4 cm high) in 1 cm of distilled water. At this depth, UV transmission was greater than 99% (91). Therefore, the incident UV intensity on the water was equated with the energy penetrating to the samples. The vessel, which accommodated up to 10 slides at one time, was positioned on the target plane 47.6 cm from the lamps in an area in which the incident radiation varied less than 5%. Intensities were measured with the UV sensitive cell prior to and during each experiment. Under these conditions the incident intensity on the surface of the water varied from 25.9 to 25.5 ergs/mm^2/sec.

For exposure to UV radiation, the slides were removed from the growth medium, rinsed in distilled water and placed into the perspex radiation vessel. Two slides were irradiated for each exposure time, which ranged from 1 to 60 min. Unirradiated controls kept in distilled water for the duration of the radiation period showed normal proliferative capacity. Following exposure the samples

were returned to the culture vessels. Irradiated and control samples were grown in separate vessels to eliminate error in survival determinations which could be introduced from resporulation from surviving filaments. In preliminary experiments it was found that resporulation could account for population increases of up to 5% which could influence survival values at high UV doses.

G. Photoreactivation

Two "daylight" fluorescent lamps(c) mounted side by side on a light table were used as the source of photoreactivating light. Immediately following exposure to a single dose of UV, the irradiated and control slides were placed on the light table in the culture vessels and illuminated at an intensity of about 1000 ft-c, for ½ to 3 hr. Following illumination, the vessels were transferred to the temperature controlled light bath, and kept there for the remainder of the 5 day growing period.

Photoreactivation under the lighting conditions encountered during routine growing procedures was also investigated. Irradiated and control samples were incubated in the dark at 22 ± 0.5°C for ½ to 9 hr immediately following irradiation and then transferred to the normal lighting conditions for the duration of the growing period.

After 5 days, samples from both procedures were analysed, and the cell survival, using the criterion to be described, was measured as a function of type and

duration of post-irradiation treatment. The survival values were compared to the value obtained when cells were irradiated with the same UV dose but grown under normal lighting conditions for the 5 day growing period.

H. Determination of the Criterion for Measurement of Proliferative Capacity

The radiosensitivity of O. cardiacum cells was measured by the loss of proliferative capacity. To determine the criterion for retention of proliferative capacity samples were irradiated at different cell ages in the first generation cycle, incubated for 5 days under the conditions previously described and then analysed microscopically. The number of cells in each filament was counted, and histograms of the percentage of filaments versus the number of cells per chain plotted for different cell ages and UV doses. By assessing the distribution of the chains in comparison to the histograms of the control samples, it was possible to determine the dividing line between survivors and non-survivors. The value of this dividing line was used as the criterion that a spore had retained its proliferative capacity. The percentage of cells surviving UV irradiation was then determined for different UV doses and cell ages, and the log percent survival plotted as a function of UV dose in ergs/mm^2.

CHAPTER II

RESULTS

A. Variations in Cell Synchrony, Cell Viability and Mean Generation Time

Differences in the degree of cell synchronization could be a source of difficulty in interpreting the experimental data. For this reason it was desirable to adopt a procedure for estimating the degree of cell synchronization of each population. Using the formula developed by Zeuthen (87) for the percent phasing, namely:

$$\text{Percent phasing} = \frac{r - T}{r} \times 100$$

where r = one-half of the mean generation time G. G was measured from the mid-point of the collection period to when 50% of the viable population, as determined from the plating efficiency, had divided. T was considered as the time interval from when 25% of the cells had divided to when 75% had divided. Both r and G were determined from the growth curve in which the percent of cells divided was plotted as a function of time after the mid-point of the collection period as shown in Fig. 2.

For a cell population which divides with perfect synchrony, a percent phasing of 100% would be obtained. Since there is some spread in cell age during the spore collection and also since the rate of movement of cells through the cell cycle towards mitosis is not identical a phasing index of 100%

FIG. 2

Percentage of cells that have divided once versus time measured in hours from mid-point of one-hour collection period. Estimated values of the plating efficiency and percent phasing are 97% and 69% respectively. The probable error of each point has been indicated by a vertical bar.

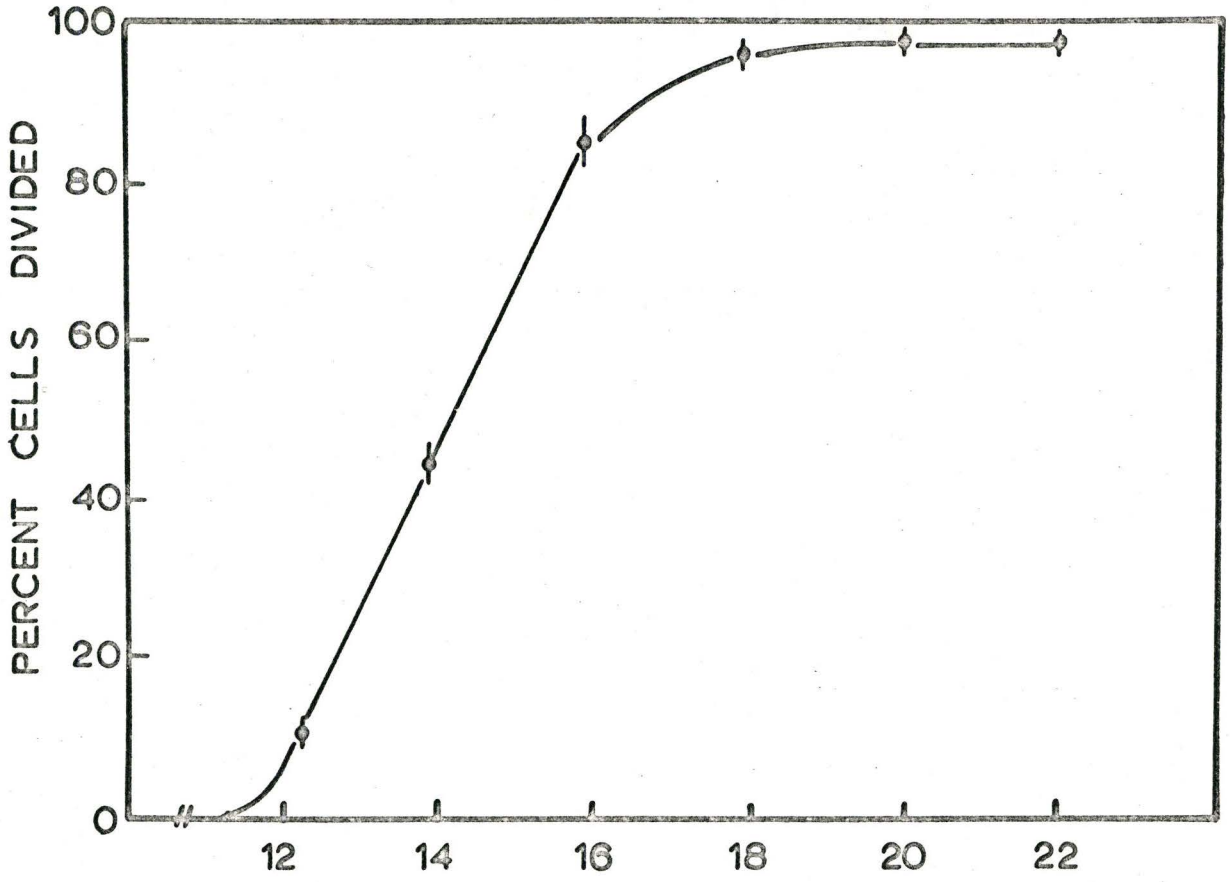
100
80
60
40
20
0
PERCENT CELLS DIVIDED
12
14
16
18
20
22
TIME IN HOURS AFTER MID POINT OF COLLECTION PERIOD

is not realized. In the present investigation the percent phasing had a mean value of 65%, however, values as high as 87% were obtained. The percent phasing for 15 of the experiments is shown in column 4 of Table I.

Another source of difficulty could arise from variations in cell viability. In column 2, Table I, the plating efficiency which was estimated from the plateau region of the 22 hr growth curve (Fig. 2) is tabulated for the same experiments. The percent maximum cells divided in the plateau region correlated well with cell viability after 5 days. The average plating efficiency was 91% and varied between limits of 82 and 99%.

A third source of difficulty could arise from differences in the rate of movement of cells through the cell cycle from one experiment to another. The mean generation time as shown in column 3, Table I varied between 15.5 and 18.5 hr. An attempt was made to normalize each generation time to a standard generation time of 16.8 hr. The value of 16.8 hr is the average generation time of all the experiments. Each time in a given experiment was multiplied by a correction factor T' determined by the relation:

$$T' = \frac{16.8}{G}$$

where G = the mean generation time of a particular experiment. Values of T' are tabulated in column 6, Table I. The use

TABLE I

Synchrony and Growth Parameters for *O. cardiacum* Cells

Expt.	Plating Efficiency (P.E.) %	Mean Generation Time (G) hr	Percent Phasing (P.I.) %	Time for 50% of the Cells to Divide (T) hr	Correction Factor (T')
(1)	(2)	(3)	(4)	(5)	(6)
1	99	16.0	73	2.2	1.05
2	90	16.6	60	3.3	1.01
3	95	16.9	87	1.0	0.99
4	94	15.4	69	2.4	1.09
5	91	15.8	73	2.4	1.06
6	87	16.5	55	3.7	1.02
7	84	16.2	53	3.8	1.04
8	82	16.7	55	4.0	1.01
9	97	16.3	71	2.4	1.03
10	87	18.4	70	2.8	0.91
11	83	15.8	59	3.2	1.06
12	92	18.0	70	2.7	0.93
13	98	17.7	65	3.1	0.95
14	98	18.0	69	2.8	0.93
15	88	17.0	68	2.7	0.99

of a correction factor may not be entirely correct since it assumes that any deviation in a particular experiment from the mean generation time (16.8 hr) is spread uniformly throughout the cell cycle. That is, it is assumed that the stages G_1, S and G_2 are uniformly lengthened or shortened depending on the value of T', or that any particular time at which the cells were irradiated is either increased or decreased depending on the value of T'. The maximum change in time amounted to less than 10% of the generation time. The overall shape of the radiosensitivity curve was not changed appreciably by these corrections.

The variation in the mean generation time (15.5 to 18.5 hr) is similar to that observed by Banerjee and Horsley (88) for O. cardiacum cells cultured in Molisch's inorganic medium (16 to 20 hr) under environmental conditions similar to those used in the present investigation. They measured the period of DNA synthesis by autoradiography during the first cell cycle of cells obtained from similar stock cultures as used in the present investigation, and estimated the lengths of the 4 cell stages to be as follows: G_1, $3\frac{1}{2}$ hr; S, 6 ± 1 hr; G_2, $6\frac{1}{2} \pm 1$ hr, and M, 2 hr. Since the mean generation time for cells grown in Molisch's inorganic medium is similar to that observed in the present experiments for O. cardiacum cells grown in Machlis' inorganic medium, the positions of the 4 cell stages are assumed to be the same.

B. Determination of the Criterion for Measurement of Proliferative Capacity

Fig. 3 shows the normal growth curve of unirradiated cells in which the log of the average number of cells per chain is plotted at increasing time following the mid-point of the spore collection period. Normal growth after about 24 hr is exponential up to 5 days and the doubling time is about 17 hr. In this particular experiment, the percentage of cells unable to divide once remained relatively constant after the first day and represented less than 5% of the total population. Early in the studies, normal growth of the spores was examined in soil extract and Machlis' medium both with and without CO_2. Using Machlis' medium or soil extract no appreciable difference was detected in the shape of the growth curve when the media was bubbled with 1% or 3% CO_2 in air or not bubbled. Since Machlis' medium is well defined in comparison to soil extract, it was decided to carry out the experiments in this medium without CO_2 bubbling.

Fig. 4 is a histogram of control samples and samples irradiated at 8 hr with increasing UV dose. To facilitate counting, filaments of more than 19 cells have been scored as 20+. In the control sample of 1090 spores, only 2.2% of the spores were unable to divide once and less than 3% of the filaments had less than 19 cells. In the UV-radiated samples, the number of 20+ filaments decreased rapidly with increasing dose while the number of short filaments

FIG. 3

Average number of cells per chain versus time from mid-point of one-hour collection period for untreated sporelings grown under normal conditions. The probable error of each plot has been indicated by a vertical bar.

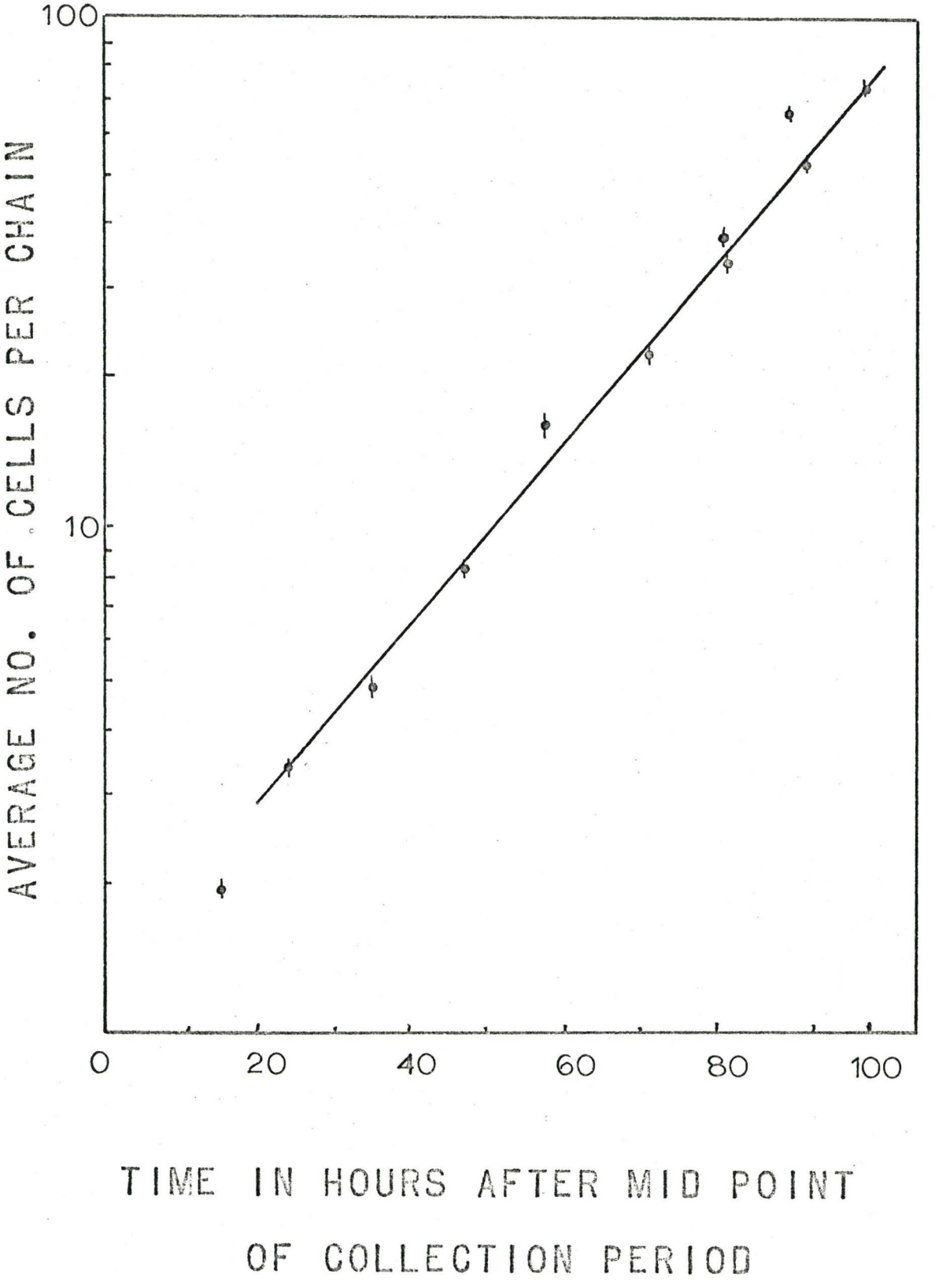
100
10
AVERAGE NO. OF CELLS PER CHAIN
0
20
40
60
80
100
TIME IN HOURS AFTER MID POINT
OF COLLECTION PERIOD

Fig. 4

Histograms of the number of cells per chain in control samples and samples irradiated with increasing UV dose at cell age 8.0 hr (S).

A.	UV dose	control
	Number of chains counted	1090
	Cells per chain	19.5 *
B.	UV dose	3064 ergs/mm^2
	Number of chains counted	2128
	Cells per chain	5.5
C.	UV dose	6130 ergs/mm^2
	Number of chains counted	2400
	Cells per chain	1.8
D.	UV dose	9194 ergs/mm^2
	Number of chains counted	1717
	Cells per chain	1.8

* Filaments of more than 19 cells have been scored as 20+.

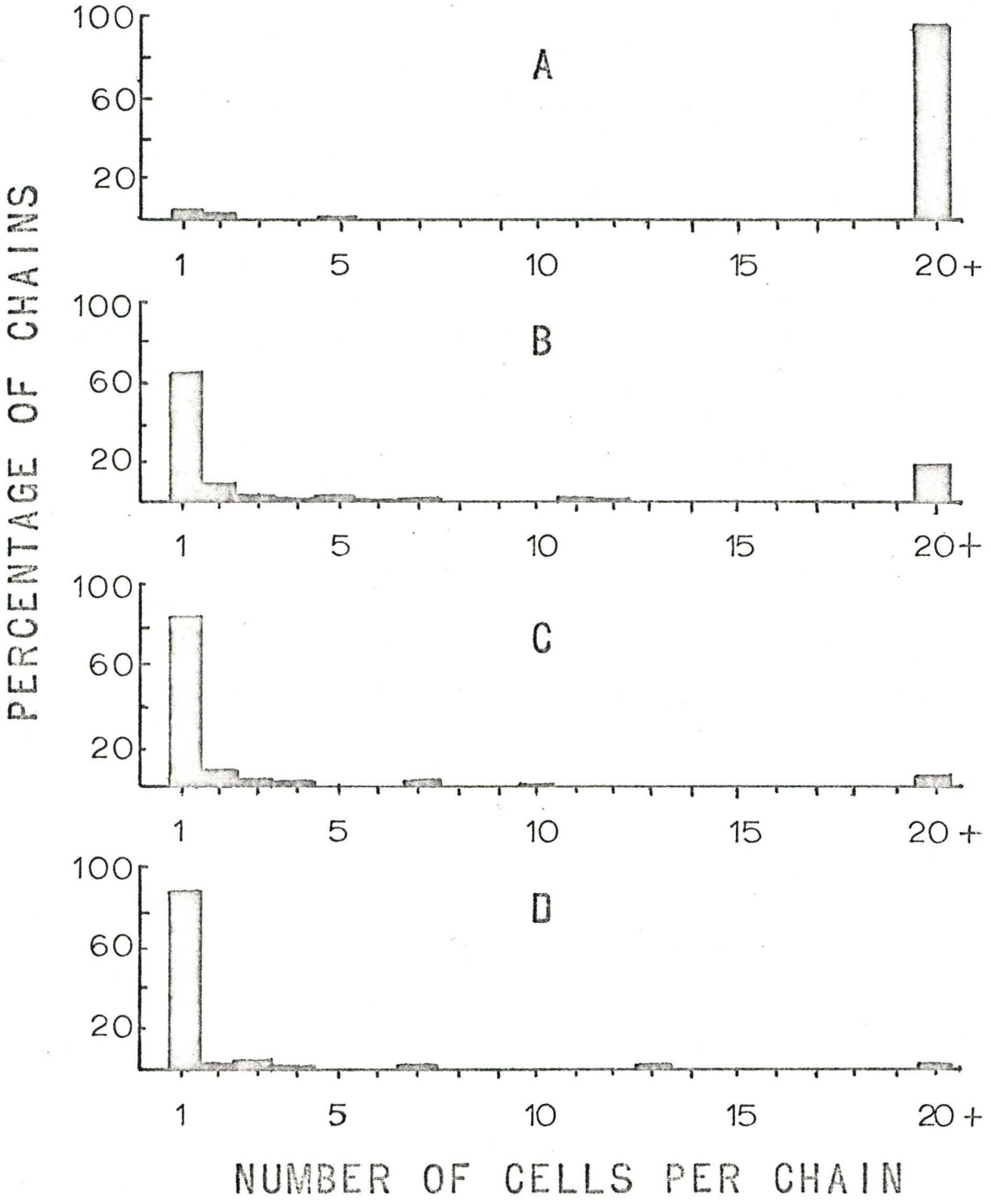
PERCENTAGE OF CHAINS
100
60
20
A
1
5
10
15
20+
B
C
D
NUMBER OF CELLS PER CHAIN

(primarily 1 cell long) increased. At each dose spores unable to divide once accounted for the largest percentage of filaments with less than 19 cells. The remainder of the filaments in the 2 to 19 cell group were mainly less than 12 cells in length.

Fig. 5 is a histogram of control samples and samples irradiated with 3064 ergs/mm^2 but at different cell ages. The general behavior of irradiated cells is similar to that shown in the previous histogram in that the length of the filament is either short (under 12 for the most part) or relatively long (beyond 19). The percentage of filaments with 19 or more cells is seen to decrease with increasing cell age at 3, 6, 10 and 13 hr respectively. As in the previous histogram, most of the short filaments were one cell in length.

In previous experiments with ionizing radiation carried out in this laboratory (77), the criterion chosen for retention of proliferative capacity was based on spores which gave rise to a filament with more than 12 cells after a 5 day post-irradiation growing period (72). Since there are relatively few chains with 8 to 20 cells, the same boundary criterion for survival, namely 12 cell long filaments, as used in the ionizing studies was adopted for the UV studies.

C. Dosimetry

(a) Distribution of UV radiation

Iso-intensity plots of UV radiation dose in the target

Fig. 5

Histograms of the number of cells per chain in control samples and samples irradiated with a UV dose of 3064 ergs/ mm^2 at different cell ages.

A.	Cell age (control)	4.5 hr
	Number of chains counted	1084
	Cells per chain	19.6 *
B.	Cell age	3.0 hr
	Number of chains counted	954
	Cells per chain	13.0
C.	Cell age	6.0 hr
	Number of chains counted	2266
	Cells per chain	7.0
D.	Cell age	10.0 hr
	Number of chains counted	1760
	Cells per chain	2.7
E.	Cell age	13.0 hr
	Number of chains counted	2001
	Cells per chain	3.2

* Filaments of more than 19 cells have been scored as 20+.

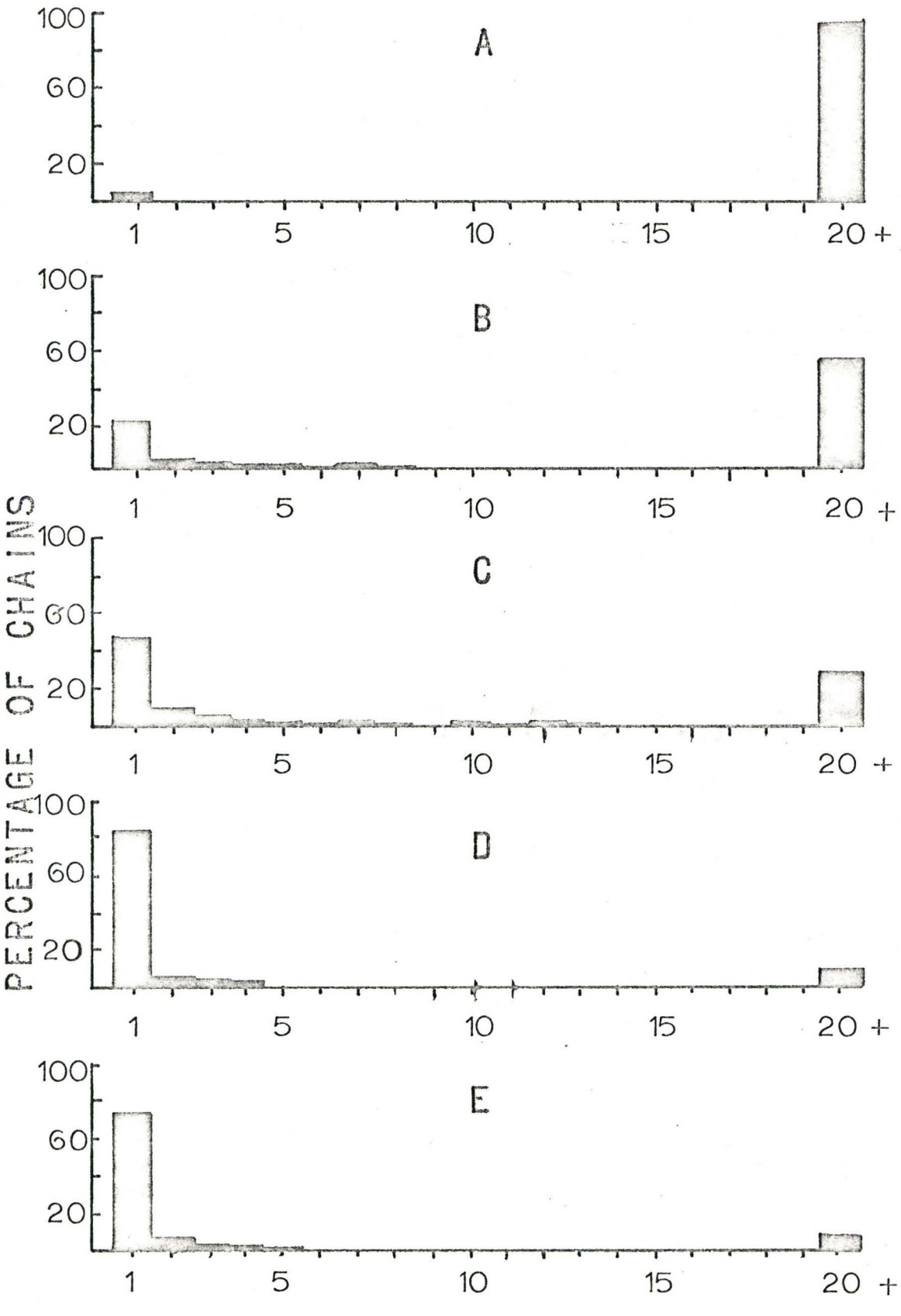
A
B
C
D
E
100
60
20
1
5
10
15
20 +
PERCENTAGE OF CHAINS
NUMBER OF CELLS PER CHAIN

plane were made to assure a uniform dose was delivered to all samples. In Fig. 6, the 95 and 90% isodose curves are shown. The center of the target plane has been represented by a cross (+). Since the surface area of the sensor cell was 4 x 2 cm, each point on the plot represents the average photon flux over an area of 8 sq cm. The relative readings at each point have been expressed as a percentage of the maximum. Measurements were taken over the entire 31 x 37.4 cm radiation surface with the long axis of the sensor cell parallel and perpendicular to the lamps. Readings made with the long axis perpendicular are plotted using the left ordinates and those with the long axis parallel using the right ordinates. From Fig. 5, the area over which the incident intensity varied less than 5% was approximately a circle of radius 8.8 cm.

(b) Intensity of UV Radiation

The absolute intensity of the UV radiation was determined by 3 different methods at 71 cm from the lamps. As outlined earlier, the sensor cell was calibrated by the manufacturer within $\pm$ 5%. The reliability of this calibration was verified by using ϕx-174 bacteriophage as a biological dosimeter. Furthermore, the UV intensity was calculated from data supplied by the manufacturer of the lamps.

Survival of the plaque-forming ability of ϕx-174 on E. coli C was determined after increasing UV exposures

FIG. 6

Iso-intensity plots of the relative UV radiation incident at various points on the target plane. The 90 (radius 12 cm) and 95% (radius 8.8 cm) iso-intensity curves are shown. The center of the plane has been represented by a cross. The lamps are positioned 47.6 cm above the center of the plane and parallel to its long axis.

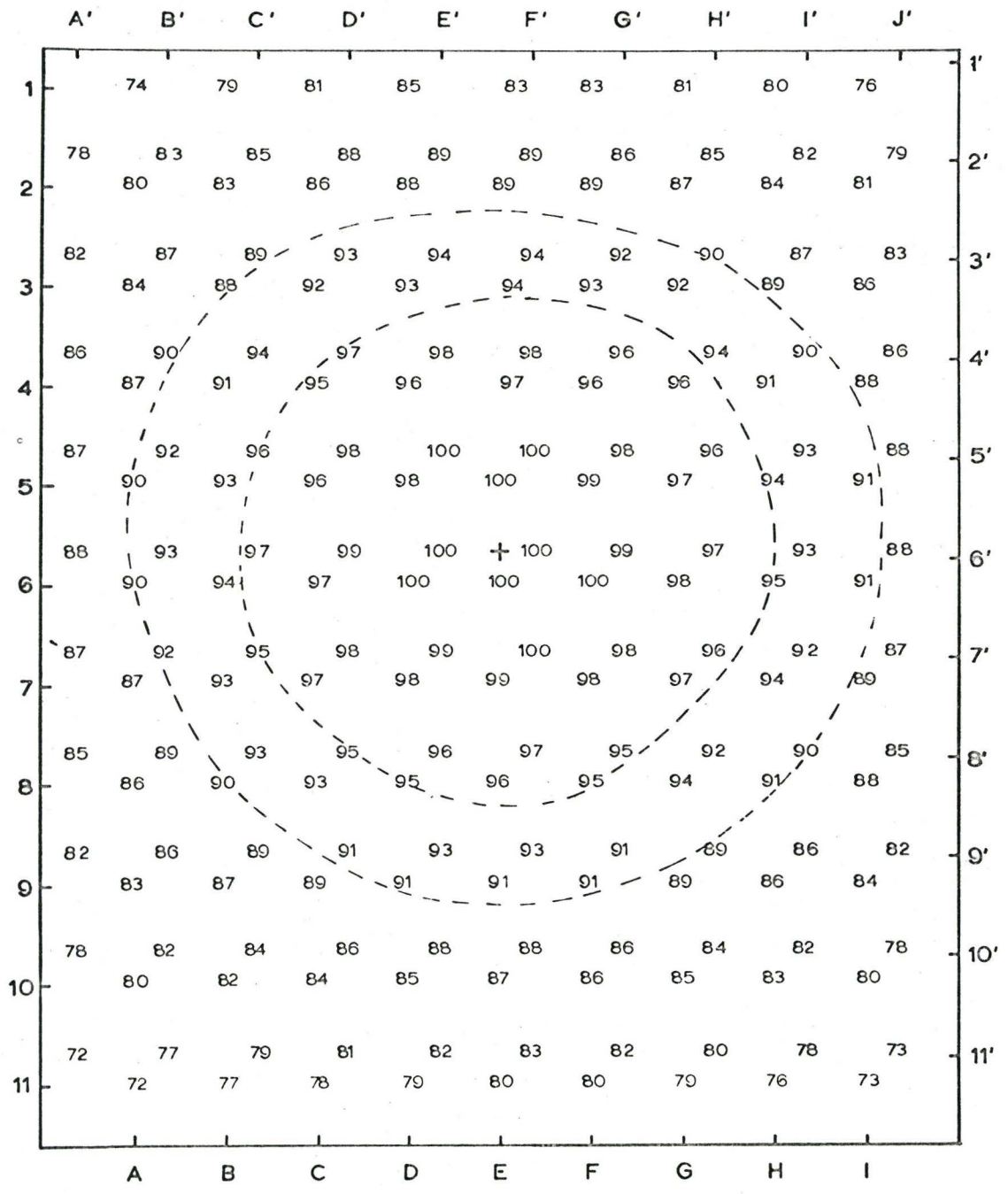
A' B' C' D' E' F' G' H' I' J'
1 74 79 81 85 83 83 81 80 76 1'
2 78 83 85 88 89 89 86 85 82 79 2'
2 80 83 86 88 89 89 87 84 81
3 82 87 89 93 94 94 92 90 87 83 3'
3 84 88 92 93 94 93 92 89 86
4 86 90 94 97 98 98 96 94 90 86 4'
4 87 91 95 96 97 96 96 91 88
5 87 92 96 98 100 100 98 96 93 88 5'
5 90 93 96 98 100 99 97 94 91
6 88 93 97 99 100 100 100 99 97 93 88 6'
6 90 94 97 100 100 100 98 95 91
7 87 92 95 98 99 100 98 96 92 87 7'
7 87 93 97 98 99 98 97 94 89
8 85 89 93 95 96 97 95 92 90 85 8'
8 86 90 93 95 96 95 94 91 88
9 82 86 89 91 93 93 91 89 86 82 9'
9 83 87 89 91 91 91 89 86 84
10 78 82 84 86 88 88 86 84 82 78 10'
10 80 82 84 85 87 86 85 83 80
11 72 77 79 81 82 83 82 80 78 73 11'
11 72 77 78 79 80 80 79 76 73
A B C D E F G H I

measured in sec. Fig. 7 shows the dose response curve obtained when the log percent survival was plotted as a function of dose in sec. Each point represents the average survival for 3 separate experiments. The Do value determined from the graph is 7.5 sec. Assuming that the Do value for survival of ϕx-174 bacteriophage is 85 ergs/mm^2 (91), the exposure rate for ϕx-174 bacteriophage irradiated in PBS was 11.3 ergs/mm^2/sec.

The calculated intensity was determined from the intensities quoted at different distances for the lamp by the manufacturer. These intensities represented average values at 100 hr lamp life.

The UV intensity at the exposure distance, 71.0 cm, as measured by each procedure is given in Table II. The UV meter value of 9.6 ergs/mm^2/sec is in excellent agreement with the calculated value of 9.4. The intensity value determined by the biological dosimeter, 11.7, is about 25% higher. The reliability of the 11.7, intensity value is of course dependent on the accepted Do value for ϕx-174. Different Do values in the range 80 to 90 ergs/mm^2 have been obtained by other workers (60, 67, 92).

It was decided to use the UV meter as a reliable method for determining the UV intensity prior to and during each experiment since the intensity value determined by the meter was in good agreement with both the calculated value and the value determined by the bacteriophage.

FIG. 7

Dose response curve for øx-174 bacteriophage irradiated in PBS at 71.0 cm distance from 2 - 15 watt germicidal lamps. The Do is 7.5 sec.

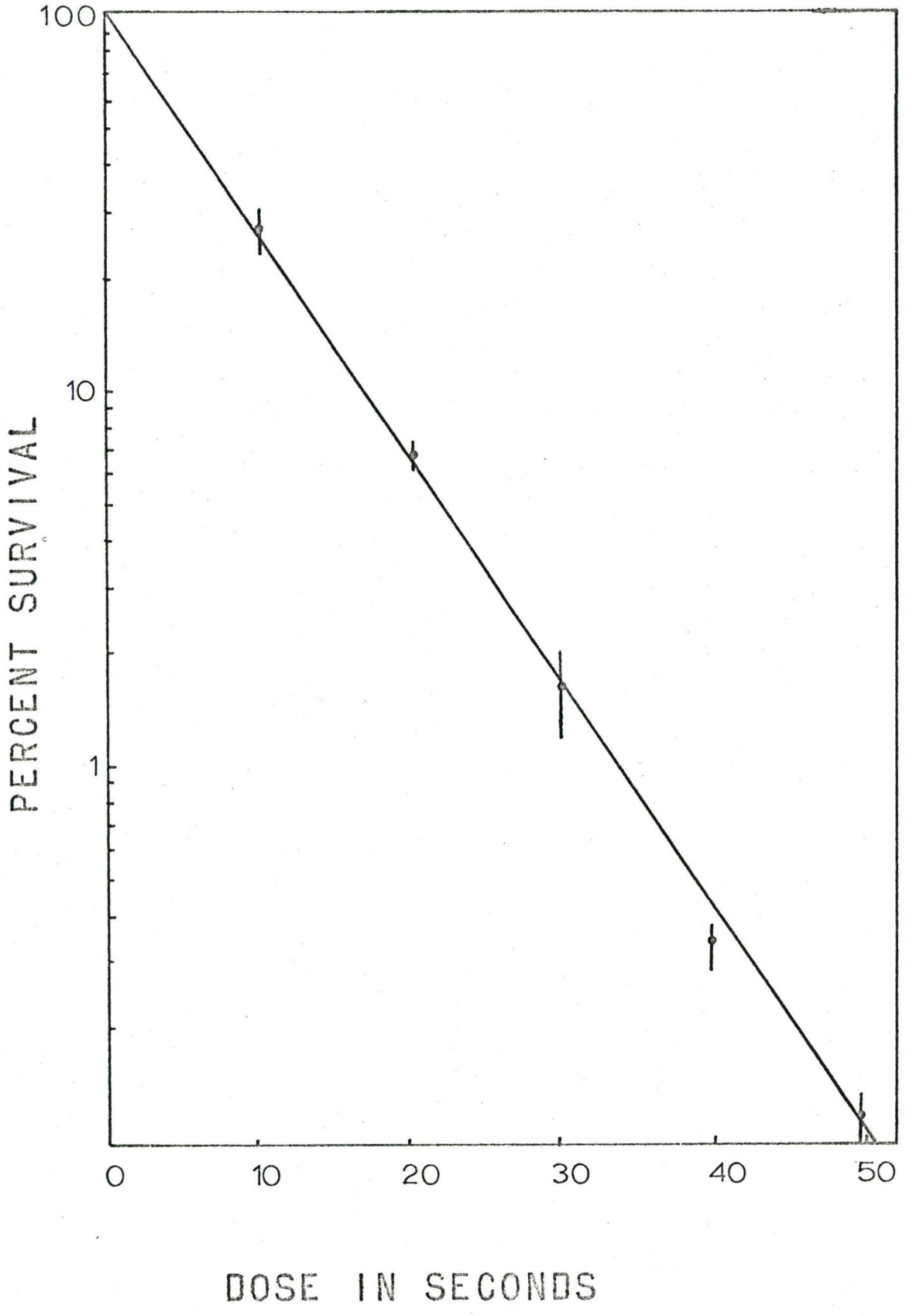
100
10
1
PERCENT SURVIVAL
0
10
20
30
40
50
DOSE IN SECONDS

TABLE II

UV Intensity at 71.0 cm from 2 — 15 Watt Germicidal Lamps

Procedure	Incident Intensity ergs/mm^2/sec
UV Intensity Meter	9.6 ± 0.5
øx-174 Bacteriophage	11.7 ± 0.4
Calculated Data (General Electric Co.)	9.4

For the experiments to be reported, the samples were positioned at 47.6 cm from the lamps and the UV meter was used to determine the absolute intensity of the UV radiation. The samples were irradiated in an open perspex vessel covered with 1 cm of distilled water (91). No correction was made for the small (less than 1%) UV absorption in the distilled water.

D. UV Radiation Experiments

(a) Survival Curves

Fig. 8, shows a detailed example of a dose-survival curve of O. cardiacum irradiated with increasing UV dose at cell age 8 hr. The experimental points in this graph were determined from 2 separate experiments. The zero dose survival has been normalized to 100%, and other values corrected by the normalizing factor. The survival curve has a complex shape consisting of an initial small shoulder followed by a rapid fall off until a dose of 17 K ergs/mm^2. Beyond this dose a second shoulder region appears extending to 30 K ergs/mm^2. The curve then falls off rapidly to the maximum dose used, 66 K ergs/mm^2. The straight line portions of the log plot indicate 2 regions of exponential decline which suggest the presence of a population of cells composed of at least 2 groups with different radiation sensitivities. The largest (90%) and most sensitive group is inactivated first and is represented by the small initial shoulder and rapid decline. The

FIG. 8.

Dose response curve of synchronously growing Oedogonium cardiacum cells irradiated with increasing UV dose at cell age 8 hr (S stage). The results from two experiments have been combined. The data for the initial portion of the dose response curve was fitted by regression analysis*. The standard errors of the Do and n values of this portion are indicated. The initial portion of the curve which represents the response for 89% of the total population has been replotted two decades lower after normalizing to 100%. Standard deviation have been indicated on the plots as vertical bars. These were determined from the relation $\sqrt{\frac{pq}{n}}$ (104) where p is the percent survival; q, the percent non survival and n, the number of filaments counted.

* Standard computer programme designed for such analysis.

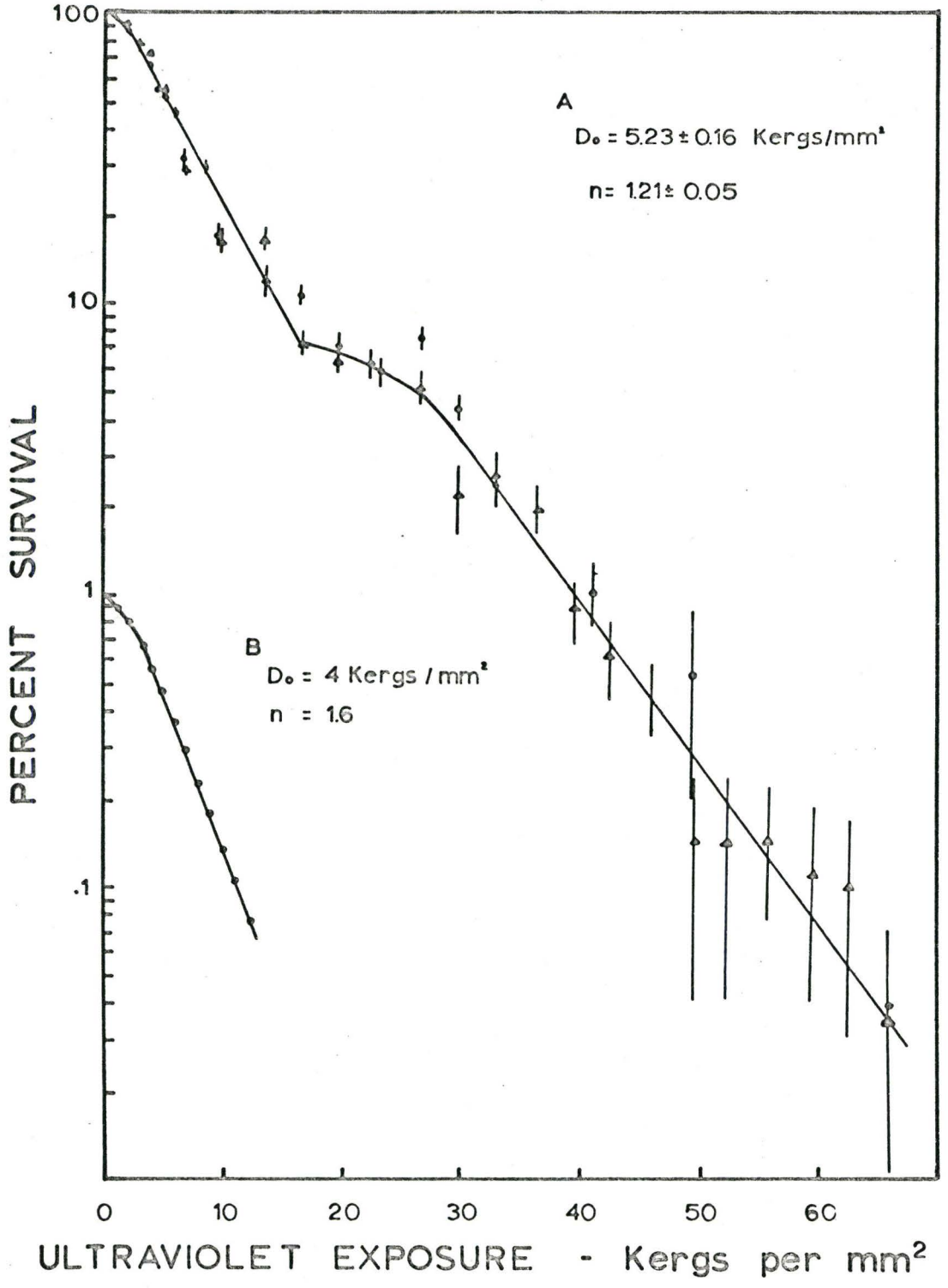
100
10
1
.1
PERCENT SURVIVAL
A
D₀ = 5.23 ± 0.16 Kergs/mm²
n= 1.21± 0.05
B
D₀ = 4 Kergs / mm²
n = 1.6
0
10
20
30
40
50
60
ULTRAVIOLET EXPOSURE - Kergs per mm²

lower portion of the curve represents the response of the smaller (10%) group which is more resistant.

The survival curve parameters, Do and $n^{(g)}$, have been determined for both components of the survival curve. The second shoulder of the complex curve was extrapolated to the zero ordinate axis, and this extrapolated shoulder region was subtracted from the measured values of the initial portion of the curve. The intercept on the ordinate axis indicates the size of the latter component in the total population. Both components were normalized to 100% and the values of n and Do determined. The normalized survival curve for the initial portion is shown 2 decades lower in Fig. 8. For the initial component, Do and n are 4.0 K ergs/mm^2 and 1.6 respectively. For the latter component these values are 7.6 K ergs/mm^2 and 15 respectively.

In most of the measured survival curves, the latter component is not as clearly defined as it is in the detailed survival curve just described. Since errors in the extrapolation of this shoulder region result in concomitant errors in the determination of the Do and n values of the initial portion of the curve, the Do and n values that will be presented as a function of cell age have been determined both with and without subtracting the extrapolated shoulder region.

(g) n, or the extrapolation number, is the number obtained when the exponential portion of the survival curve is extrapolated back to zero dose.

Fig. 9 shows dose response curves measured for a cell population divided into 6 groups, with each group irradiated at a different cell age in the first generation cycle. These curves have been analysed in the manner described above. The Do and n values quoted in Fig. 9 are those for the initial portions of the curves without subtracting the values of the extrapolated shoulder region. At each cell age the latter component comprises about 10% of the total population. In addition, the Do value of this component is similar to that of the initial component at each cell age.

(b) Variations in Sensitivity During the Generation Cycle

In Fig. 10, the Do values for the initial components of the dose-response curves have been plotted for increasing cell age both with (dotted line) and without (solid line) subtracting the extrapolated shoulder region. The positions of the different cell stages G_1, S, G_2 and M of an unirradiated control culture are indicated.

For both curves, the Do value increases during G_1 reaching a peak during mid S ($5\frac{1}{2}$ to 6 hr) indicating the time of maximum UV resistance. After this time a rapid decrease in the value of Do occurs as the cells progress further through the cell cycle until the maximum sensitivity has been reached at G_2 ($12\frac{1}{2}$ hr) and M (14 hr). In both

FIG. 9

Dose response curves of Oedogonium cardiacum cells irradiated with increasing UV dose at selected times in the first generation cycle. The Do and n values shown are for the initial component of the curves without subtracting the extrapolated shoulder region.

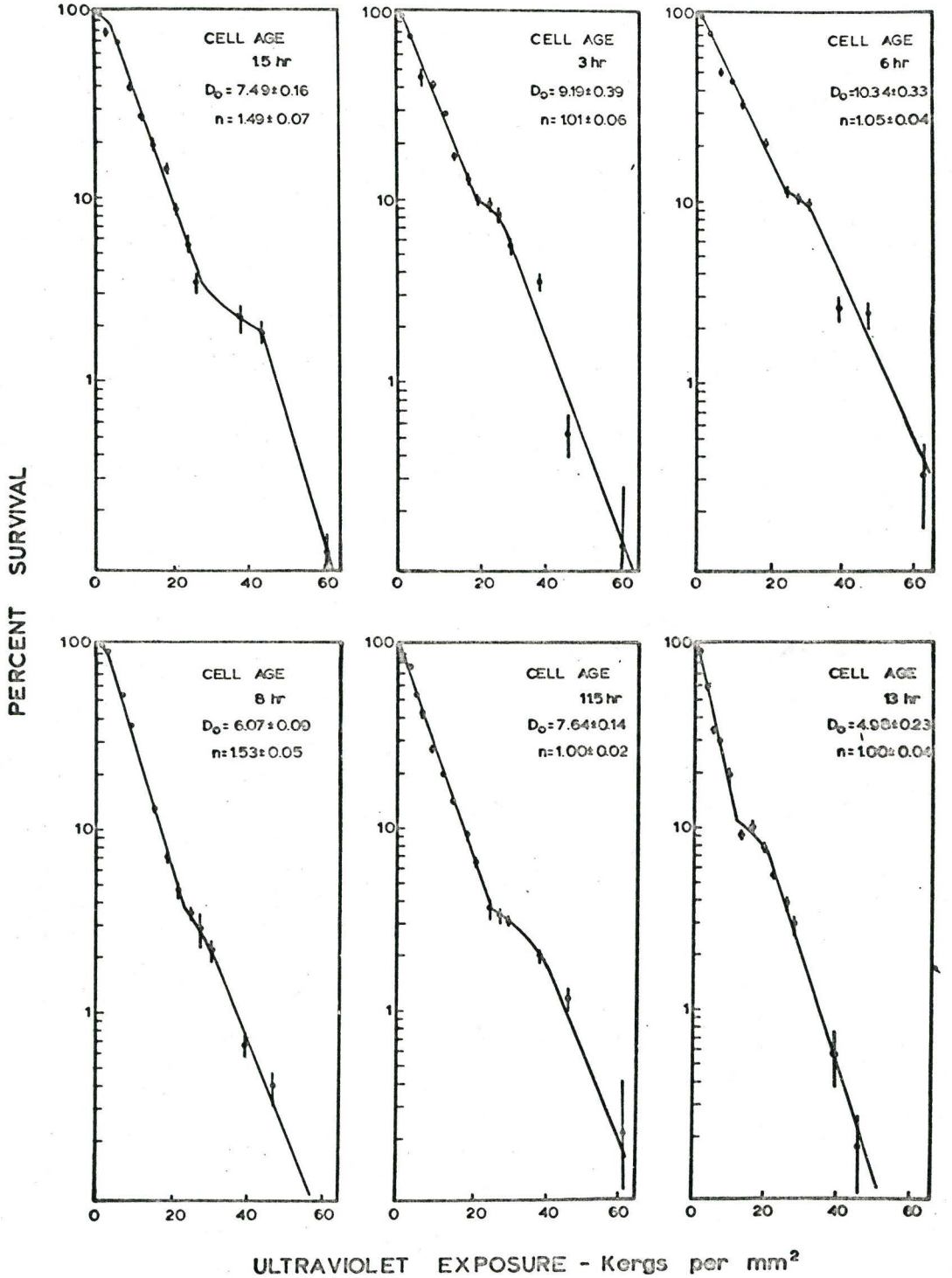
CELL AGE
1.5 hr
D_o = 7.49 ± 0.16
n = 1.49 ± 0.07
CELL AGE
3 hr
D_o = 9.19 ± 0.39
n = 1.01 ± 0.06
CELL AGE
6 hr
D_o = 10.34 ± 0.33
n = 1.05 ± 0.04
CELL AGE
8 hr
D_o = 6.07 ± 0.09
n = 1.53 ± 0.05
CELL AGE
11.5 hr
D_o = 7.64 ± 0.14
n = 1.00 ± 0.02
CELL AGE
13 hr
D_o = 4.93 ± 0.23
n = 1.00 ± 0.04
PERCENT SURVIVAL
100
10
1
0
20
40
60
ULTRAVIOLET EXPOSURE - Kergs per mm²

FIG. 10

The measured survival curve parameters, Do and n, for the initial components of the survival curves with (———) and without (----) subtracting the extrapolated shoulder region for O. cardiacum cells irradiated at various cell ages. The position of the cells in the cell cycle is also indicated.

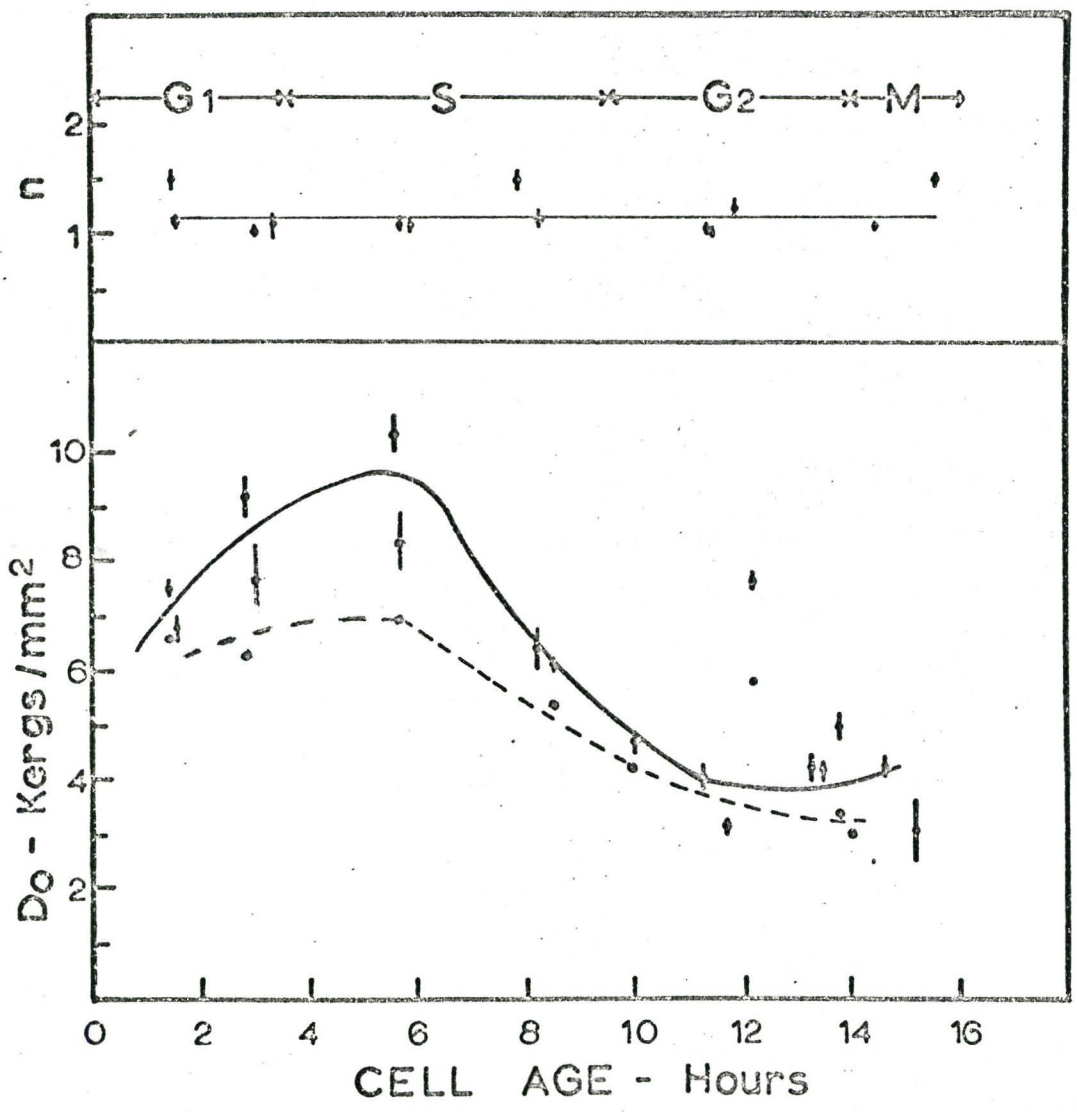
G1
S
G2
M
n
2
1
Do - Kergs/mm²
10
8
6
4
2
0
2
4
6
8
10
12
14
16
CELL AGE - Hours

curves the Do value varies by a factor of approximately 2.5 throughout the cell cycle. Thus although there is some uncertainty in the actual value of Do for the initial component due to the presence of the small (10%) apparently resistant component at each cell age measured, both methods of calculation indicate the same variation in Do with cell age.

The values of n have also been determined for the initial components of the dose response curves measured at various cell ages with and without subtracting the extrapolated shoulder region. In both cases n remains essentially constant varying between 1.0 and 1.6 throughout the cell cycle. The n values for the initial components of the survival curves without subtracting the shoulder region have been plotted in the upper half of Fig. 10.

(c) Seasonal Variations in Sensitivity During the Generation Cycle

In Fig. 11, the Do values of the initial portion of the dose response curves without subtracting the extrapolated shoulder region, have been plotted at increasing cell age in the first generation cycle for cells irradiated in the winter months (November 1, 1967 to March 1, 1968) of the experimental period (dotted line). For comparison purposes, the Do values of the initial components of the curves for cells irradiated during the remainder of the

FIG. 11

The Do values for the initial components of the survival curves without subtracting the shoulder regions for cells irradiated at various cell ages during the winter months (----) and the remainder (——) of the experimental period. The values of n for the survival curves of cells irradiated in the winter are shown in the upper half of the figure. The position of cells in the cell cycle is also indicated. The solid curve has been reproduced from Fig. 10.

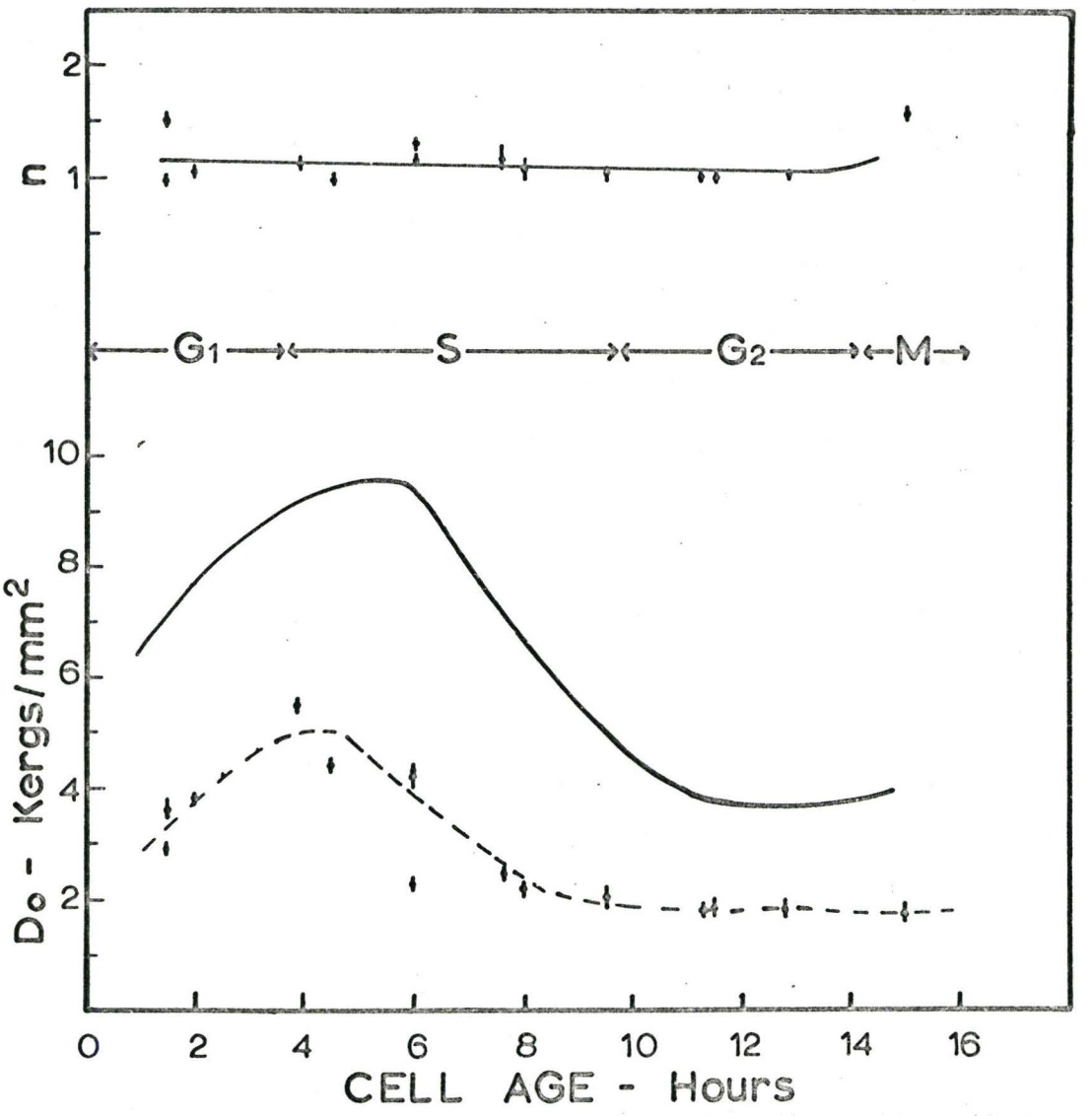
n
2
1
G1
S
G2
M
10
8
6
4
2
Do - Kergs/mm2
0
2
4
6
8
10
12
14
16
CELL AGE - Hours

experimental period (upper curve Fig. 10) have been replotted (solid line) in Fig. 11. The positions of the different cell stages of an unirradiated control culture are also indicated. Although the age dependent variation in sensitivity is about the same for each experimental period, cells irradiated during the winter period are about twice as sensitive.

The values of n for survival curves measured during the winter months were essentially constant and any changes detected varied within the same range (1.0 and 1.6) of n values obtained for the remainder of the year. These values are shown in the upper half of Fig. 11.

(d) The Radiosensitivity of Progeny from UV-Irradiated Single Cells

The "tail" on the UV response curve referred to in section (a) could be explained on the basis that about 10% or less of the cells form a component which represents a UV resistant mutant. In order to investigate this possibility single surviving chains in which the basal spores had been irradiated with 60 K ergs/mm^2 in mid S (6 hr) were individually isolated and cultured in separate jars. After a 5 month growing period the filaments were induced to sporulate in the manner previously described and the collected zoospores were irradiated. The UV radiosensitivity of these cells was measured 3 times and 2 of the survival

curves for these cells are shown in Fig. 12, for cells irradiated at mid S (6 hr). This survival curve is again complex similar to curves obtained from "normal" cultures grown from non-irradiated cells. The initial more sensitive component in Fig. 12 represents about 90% of the population as was also the case for cells from the "normal" cultures described in Figs. 8 and 9. Also the Do and n values, 3.6 K ergs/mm^2 and 1.3 are about the same as the values 3.9 K ergs/mm^2 and 1.3 respectively for cells from the "normal" cultures irradiated in the winter period (See Fig. 11). For the latter component the 2 Do values obtained are again comparable, 5.2 K ergs/mm^2 and 4.8 K ergs/mm^2.

Since the Do values of both components of the complex survival curve for cells from the cultures grown from the progeny of UV-irradiated cells are comparable to those from "normal" cultures suggests that the inflexion at 10% in the survival curve is not caused by a UV resistant mutant.

(e) Photoreactivation

A preliminary experiment was carried out to determine if photoreactivation occurred with this cell system following UV irradiation, and if so whether it

FIG. 12

UV survival curves obtained for O. cardiacum cells age 6.0 hr (S stage) collected from the progeny of a single cell which had survived a UV dose of 60Kergs/mm^2. The Do and n values shown are for the initial component of the curves without subtracting the extrapolated shoulder region.

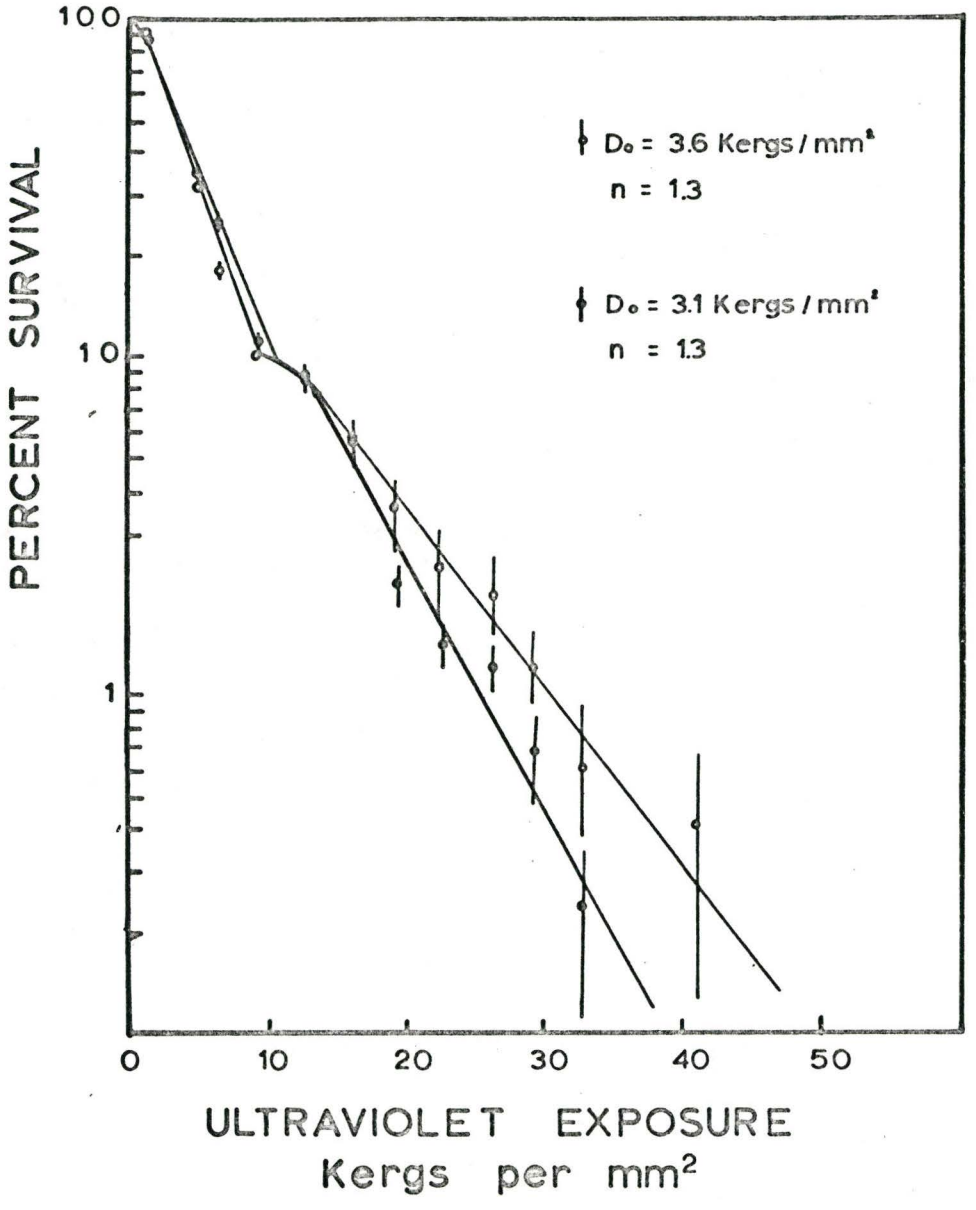
100
10
1
PERCENT SURVIVAL
D_o = 3.6 Kergs / mm²
n = 1.3
D_o = 3.1 Kergs / mm²
n = 1.3
0
10
20
30
40
50
ULTRAVIOLET EXPOSURE
Kergs per mm²

occurred under the lighting conditions used throughout this investigation. Cells which had been irradiated during S with a dose of 9780 ergs/mm^2 were divided into 2 groups. Samples in the first group were exposed to fluorescent "daylight" at an intensity of 1000 ft-c for increasing periods of time up to 3 hr and then set to grow at normal lighting conditions of 300 ft-c. Unirradiated control samples were exposed to 5 hr of this light intensity without any change in percentage survival from that of the normal controls. These results along with the percent survival at increasing times of exposure are tabulated in columns 2 and 3 of Table III. Under normal conditions at 9180 ergs/mm^2 the percent survival was 36.8%. One-half hour of exposure to the white light yielded a percent survival of 72.5%. Further exposure to white light did not change the percentage survival.

Samples from the second group of UV-irradiated cells were placed in the dark for increasing periods of time and then set to grow under normal lighting conditions. Data from this experiment are shown in columns 4 and 5 of Table III. Unirradiated samples placed in the dark for 15 hr yielded approximately the same percent survival (98) as did the controls (99). The percent survival of the UV-irradiated samples decreased from 36.8 to 15.9% for 9 hr of incubation in the dark.

The results of this experiment show that post-irradiation exposure to 1000 ft-c intensity white light results in a considerable repair of UV-induced damage as

TABLE III

Survival of O. cardiacum cells Irradiated at S Stage with a Dose of 9180 ergs/mm^2 before Photoreactivation at 1000 ft-c or Incubation in the Dark.

(1) UV Dose (ergs/mm^2)	(2) Time at 1000 ft-c (hr)	(3) Survival %	(4) Time in Dark (hr)	(5) Survival %
0	0	99 ± 0.3	0	99 ± 0.3
0	5.0	99 ± 0.3	15.0	98 ± 0.7
9180	0	36.8 ± 1.2	0	36.8 ± 1.2
9180	0.5	72.5 ± 1.4	0.5	26.6 ± 1.4
9180	1.0	73.5 ± 1.4	1.0	27.1 ± 1.2
9180	2.0	70.8 ± 1.3	2.0	19.3 ± 1.7
9180	3.0	75.9 ± 1.5	3.0	16.1 ± 1.1
9180			4.0	16.1 ± 1.1
9180			5.0	17.0 ± 1.0
9180			9.0	15.9 ± 1.2

measured by the proliferative capacity of the cells. Some of the data from Table III is plotted in Fig. 13 where the percentage survival is shown versus one-half hour exposures to white light of increasing intensity. This curve suggests that there may be some photo-reactivation occuring at our normal lighting conditions for both winter and summer grown cells.

E. Comparison of UV and X-Ray Radiosensitivity at Different Cell Ages

In Fig. 14, the Do values for cells irradiated with UV radiation (solid line and right ordinate) are compared to the values of Do determined by others (79) for cells exposed to ionizing radiation (dotted line and left ordinate) at increasing cell age. The general shapes of both curves are similar. During G_1 sensitivity to both types of radiation decreases reaching a minimum value during S at about 5.5 hr for UV and between 5 and 7 hr for x-irradiation. Sensitivity then increases reaching a maximum during late G_2 and M as indicated by the minima in the curves at 13 to 14 hr. For ionizing radiation the Do value changes by a factor of 7 from about 1000 rads at mid S to 150 rads at late G_2; however, for UV radiation the Do value changes only by a factor of 2.5 from about 9.8 K ergs/mm^2 at mid S to 3.5 K ergs/mm^2 at late G_2 and M.

FIG. 13

The percentage survival of single cells irradiated with a UV dose of 9180 ergs/mm^2 versus one-half hour exposure to different intensities of white light. The light intensity under which cultures were routinely grown is indicated.

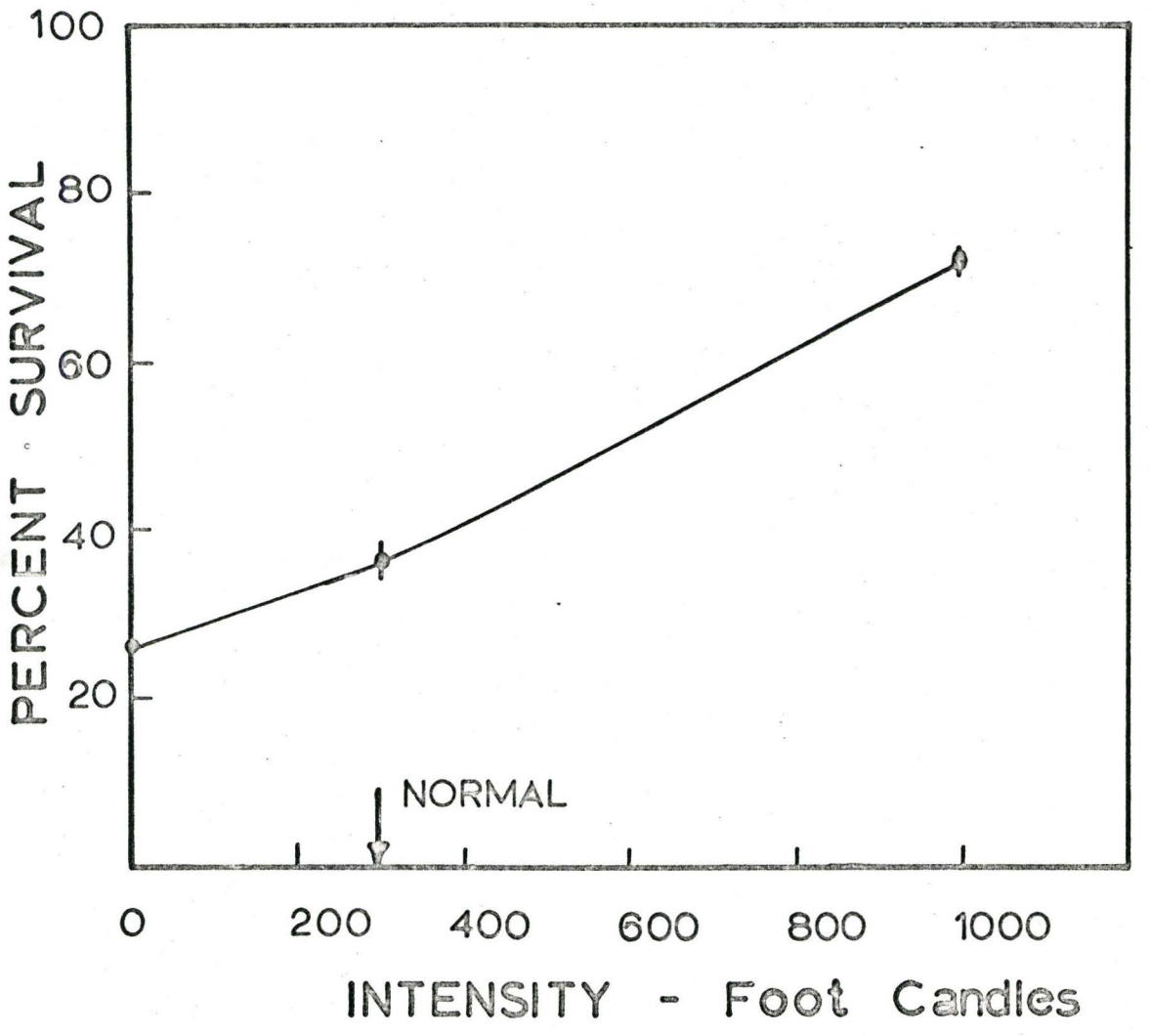
100
80
60
40
20
PERCENT SURVIVAL
NORMAL
0
200
400
600
800
1000
INTENSITY - Foot Candles

FIG. 14

Comparison of the Do values of the survival curves of cells irradiated at various cell ages with UV radiation (solid line and right ordinate) or ionizing radiation (dotted line and left ordinate) (79). The position of the cells in the cell cycle is also indicated.

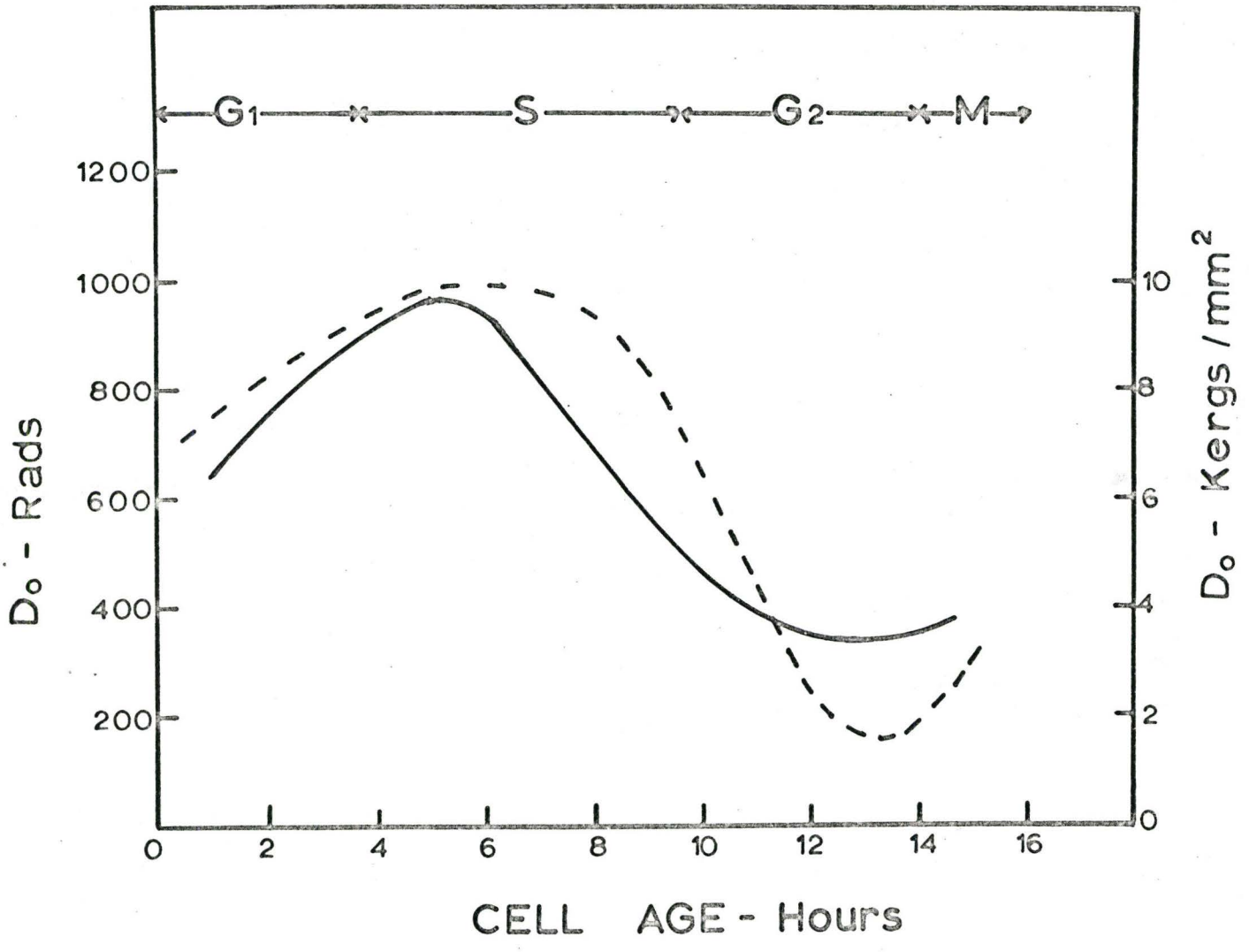
G1
S
G2
M
1200
1000
800
600
400
200
0
2
4
6
8
10
12
14
16
10
8
6
4
2
0
Do - Rads
Do - Kergs / mm2
CELL AGE - Hours

The n values for x-irradiated cells varied from 20 for G_1 cells to 40 for late S cells and then drops slowly to between 1 and 2 for G_2 and M cells. In contrast the n values for UV-irradiated cells remains relatively constant varying between 1 and 2 for all cell ages. This significant difference in response suggests that the mechanisms of action of the two types of radiation differ.

CHAPTER III

DISCUSSION

In this investigation the UV radiosensitivity, as measured by loss of proliferative capacity, of synchronously growing Oedogonium cardiacum cells was determined and correlated with the four stages, G_1, S, G_2 and M, of the cell cycle. At all stages the survival curves exhibited a complex shape indicating a population of cells heterogeneous in their radiosensitivity. The presence of a persistent shoulder at about the end of the first decade of survival suggests that the population consists of at least two components. One component is represented by the initial part of the survival curves and accounts for about 90% of the population. The other component is represented by the latter part of the curves and amounts to about 10%. The presence of this small latter component produces an uncertainty in the magnitude of the survival parameters, Do and n, for the main group of cells since it is difficult to obtain accurate survival data at high dose levels for every curve measured. Even for those curves where detailed analysis is possible there is still uncertainty in the manner of extrapolating the

shoulder region. Thus, calculations were performed in two ways to determine the Do and n values for the initial portions of the survival curves. In the one way, values were determined directly from the initial part of the curve neglecting the latter portion, and in the other way the contribution of the latter portion was first subtracted.

Although the magnitude of the Do values changed depending on the method of calculation, the change in Do with cell age was relatively the same. During G_1 the Do value increased slowly, reaching a maximum value at mid S indicating that these cells were more resistant at this particular stage. Thereafter, the Do value decreased reaching a minimum value at late G_2. From the middle of S to the end of G_2 there occurred a 2.5 fold change in radiosensitivity. In contrast, the value of n remained relatively constant varying between 1.0 and 1.6 for both methods of calculation.

In Table IV the UV radiosensitivity of O. cardiacum is compared to the radiosensitivity of seven other cell lines. Data on the UV radiosensitivity of yeast, bacteria and fungus is also included in the table. The stages of the cell cycle have been determined for only five of the cell lines: D98/AG cells, mouse L cells, Chinese hamster cells, human epithelial kidney cells and HeLa cells. Therefore it is only possible to compare O. cardiacum

TABLE IV

The UV Radiosensitivity of Cells at Different Stages of the Generation Cycle

Cell Line	Radiosensitivity	Investigator
Saccharomyces cerevisiae	Resistant - during mitosis Sensitive - interdivisional period	Elkind and Sutton (74) 1959
Schizosaccharomyces pombe	Resistant - during gene replication Sensitive - during and immediately after nuclear division	Swann (68) 1962
Eschericha coli	Resistant - during mid cell cycle and prior to nuclear division Sensitive - immediately after nuclear division	Helmstetter and Uretz (73) 1963
Ustilago hordei	Resistant - prior to and following DNA synthesis Sensitive - during DNA synthesis	Hood (66) 1968
Human cell line D98/AG	G_1 - most sensitive mid S - most resistant G_2 - decreased resistance	Erikson and Szybalski (75) 1963
Chinese hamster cells	G_1 - Do = 39 ergs/mm^2 n = 3 early S - Do = 34 ergs/mm^2 n = 12 late S Do = 72 ergs/mm^2 early G_2 n = 3	Sinclair and Morton (46) 1965
Mouse L cells	G_1 - Do = 45 ergs/mm^2 D_{37} (h) = 125 ergs/mm^2 S - Do = 70 ergs/mm^2 D_{37} = 250 ergs/mm^2 late S Do = 80 ergs/mm^2 early G_2 D_{37} = 290 ergs/mm^2 M - Do = 75 ergs/mm^2 D_{37} = 200 ergs/mm^2	Rauth and Whitmore (67) 1966

Cell Line	Radiosensitivity	Investigator
HeLa cells	G_1, G_2 } most resistant S most sensitive	Djordjevic and Tolmach (47) 1967
Human epithelial kidney cells	G_1, G_2 } most resistant S most sensitive	Scaiffe and Brohee (65) 1968
Chlamydomonas reinhardii	early cell stage - Do = 2.1 K ergs/mm^2, n = 10 DNA synthesis - Do = 4.6 K ergs/mm^2, n = 4 (assumed) before meiosis - Do = 3.1 K ergs/mm^2, n = 1	Davies (26) 1965
Blastocladiella emersonii	G_1 (assumed) Do = 87 ergs/mm^2 S and G_2 (assumed) Do = 213 ergs/mm^2	Deering (61) 1968
Oedogonium cardiacum	G_1 - Do = 7.5 K ergs/mm^2 S - Do = 9.5 K ergs/mm^2 G_2 - Do = 4.0 K ergs/mm^2 M - Do = 4.2 K ergs/mm^2	Parker 1969

(h) D_{37} - the UV dose necessary to reduce the percentage survival to 37% of the initial value.

with respect to stage UV radiosensitivity to these five cell lines. The first three of the cell lines were found to be most resistant to UV radiation during S, in agreement with the response for O. cardiacum. In contrast human epithelial cells and HeLa cells were found to be most resistant during G_1 and G_2. For mouse L cells, Chinese hamster cells and D98/AG cells maximal sensitivity occurs in G_1. Maximal sensitivity for human epithelial kidney cells and HeLa cells occurs in S. For O. cardiacum maximal sensitivity occurs in G_2. Thus there does not seem to be one cell stage for all cell lines which is either most sensitive or most resistant to UV radiation. Rauth (67) has suggested that the difference between D98/AG cells and mouse L cells may be due to differences in the radiation procedures. Furthermore, Djordjevic and Tolmach (47) question whether the behavior of the HeLa cells and mouse L cells is typical of cultured mammalian cells in general. Since differences in stage sensitivity are also seen in a similar analysis of data for radiosensitivity following ionizing radiation (102, 103) it is not unreasonable to assume that differences in stage radiosensitivity are probably due to characteristics of the different cell lines.

The data by Davies (26) and Deering (61) on the UV radiosensitivity of Chlamydomonas reinhardii and Blastochadiella emersonii respectively, does not permit a stage comparison of radiosensitivity. Experimental difficulties with these two plant systems have precluded the

determination of the S period by labelling techniques. However, both authors believe that the time of maximal resistance in their cell systems occurs during the period of DNA synthesis. Deering has suggested that in B. emersonii the period of maximal UV radiosensitivity following nuclear division corresponds to either G_1 or early S. In the diploid meiotic spores of C. reinhardii, maximal radiosensitivity occurs immediately after the onset of growth following spore production and maturation. The complexity of the division cycle of C. reinhardii precludes futher comparison with O. cardiacum. For all three plants, Do changes by a factor of about two throughout the cell cycle; however, the magnitude of the Do values differ. In O. cardiacum the Do value varies between 3 and 7 K ergs/mm^2 throughout the cell cycle which is comparable to C. reinhardii in which Do varies between 2 and 4.5 K ergs/mm^2. In contrast, B. emersonii germlings are appreciably more sensitivie since Do varies between 87 and 213 ergs/mm^2. Differences in UV cytoplasmic absorption could readily account for the apparent absolute differences in UV sensitivity.

The exact reasons for the stage dependent variations in radiosensitivity are obscure. However, three possible explanations, which are not mutually exclusive, can be considered as reasonable hypotheses for these variations. These include: (1) cyclic differences in attenuation of the UV intensity in passing through part of the cell

before reaching the target, (2) differences in the repair activities at all cell ages and (3) differences in the number or type of UV-induced photoproducts at different times in the generation cycle.

O. cardiacum cells are sufficiently large (35 μ x 105 μ) that UV radiation is attenuated by the intervening cytoplasm before it reaches the nucleus. A crude attempt has been made to measure the approximate UV attenuation in the cytoplasm between the apical cell wall and the nuclear membrane. About 60,000 cells were lysed by ultrasonication and centrifuged to precipitate the light scattering fragments. The UV absorbance at 254 mu of the supernatant containing both cytoplasmic and nuclear material was measured. From these measurements it was calculated that only about 35% of the UV radiation would penetrate the cytoplasm and reach the nucleus.

To examine whether or not variations in the position of the nucleus would explain the shape of the age response curve (Fig. 10), the distance between the outer nuclear membrane and apical cell wall was measured at different ages. These measurements are tabulated in Table A, Appendix D. Throughout the cell cycle the mean distance varies in the range 30.5 to 37.2 μ. However, the mean distance at any cell age has an appreciable standard deviation of 4 to 8 μ. This precluded the possibility of drawing any accurate correlation between the measured intervening cytoplasmic distance as a function of cell age. In addition, if one considers the increase in size of the nucleus as the cells

progress through the cell cycle (column 3, Table A), the mean distance between the apical cell wall and the center of the nucleus is relatively the same in G_1, S and early G_2 (column 5, Table A). Not until immediately before mitosis (13 to 15 hr) when the nucleus migrates apically does the distance decrease. It is unlikely that a small change in distance of the order of 4 μ could explain the 2.5 fold difference in UV radiosensitivity between G_2 and S cells. Furthermore since these distances are relatively constant for G_1, S and G_2 cells it would not explain the variations in radiosensitivity between these stages. Therefore cytoplasmic absorption can not explain the general shape of the UV radiation response. This conclusion is in agreement with similar results obtained by Deering (61). He investigaged the UV radiosensitivity of B. emersonii germlings which are also sufficiently large that UV radiation is attenuated as it passes through the cell. He found that although only 25 to 50% of the UV radiation penetrated to the nucleus, gradual variations in penetration could not explain the cyclic sensitivity changes actually observed.

The second explanation suggested for the variations in radiosensitivity throughout the cell cycle involves differences in the repair activity in the different stages of the cell cycle. Davies (26) and Kimball (49) have shown that in C. reinhardii and P. caudatum respectively, the repair activities are not the same at all cell ages. Since

photoreactivation at high intensity (1000 ft-c) white light has been observed in our system it is reasonable to hypothesize that differences in the repair activities of this mechanism at normal lighting conditions and also differences in dark repair mechanisms (45) with cell age, could be manifested as changes in radiation sensitivity. Davies (26) and Deering (61) have suggested that differences in the repair activities throughout the cell cycle could result from either: (a) differences in the concentration of the repair enzymes or the accessibility of these enzymes to the lesions at each cell age; or (b) to a more efficient repair at some cell ages because of the increased time available for repair before the damage is fixed. As shown in Fig. 10, O. cardiacum cells are most resistant to UV radiation during late G_1 and early S. Irradiation at either of these stages would allow a relatively long time to elapse before mitosis if, as indicated by others (26), mitosis is the terminal event beyond which no further repair can occur. Concomitantly, cells in G_2 would be expected to have the greatest sensitivity as the time available for repair at this stage is much shorter. It could also be hypothesized that cells irradiated in G_2 and mitosis would be more sensitive because lesions might be inaccessible to repair enzymes due to the tight coiling of the DNA. Another possible reason for the sensitivity of stages near division, which has been suggested by Davies (26), is that the rate

of fixation of lesions is accelerated at these stages. He observed that in C. reinhardii the photoreactivable sector decreased more rapidly, that is, fixation occurred at a more rapid rate after irradiation before meiosis than at the early cell stages.

At all cell ages, O. cardiacum cells unable to divide once after UV-irradiation represent the largest percentage of non-surviving cells. However, at G_1 this value was only 55% as compared to 87% at late G_2 (Fig. 5). This difference could be explained by either: (a) a difference in the number and/or type of UV-induced photoproducts at these cell stages, or (b) a more efficient repair capacity of cells in G_1 than at G_2. At the present time there is no evidence available in the literature to suggest that the UV-induced photoproducts differ throughout the cell cycle as will be discussed later. Therefore much of the variation in stage sensitivity is probably due to different repair activities. Further studies on photoreactivation and also on dark repair are planned to test this conclusion.

The third possible explanation for the variations in stage radiosensitivity, namely, differences in the number or type of UV-induced photoproducts with cell age can not be eliminated as a hypothesis at present. Donnellan et al (see review: 93) have shown that the photoproducts can vary with the physiological state of the organism and Setlow et al

(17) have shown that there is an increase in the DNA-protein cross-linking in UV resistant cells. Rauth (67) has suggested that the number of photoproducts produced may be a function of the particular state of the DNA or other sensitive targets at the time of irradiation. The possibility of the differential production of photo-products as a function of cell age is presently being investigated in other laboratories (26, 45, 67, 70).

In this investigation, evidence has been presented (Fig. 11) to show that O. cardiacum cells are more sensitive to UV radiation during the winter months (November to March) than during the remainder of the year. However, at both periods, the variation in radiosensitivity with cell age is unchanged. The seasonal difference can perhaps be explained by changes in cytoplasmic UV absorption assuming that the sensitive target is the nucleus. Stock cultures were grown for the most part on culture racks placed in a north window where there would be seasonal fluctuations in the intensity, durations and spectral distribution of the light. Since all three factors are rate limiting for photosynthesis (94), cellular constituents associated with the photosynthetic apparatus would be present in reduced amounts in winter grown cells. Stern et al (see review: 95) have shown that the amounts of chlorophyll per cell can be changed by lighting conditions in Euglena and Hill et al (95) have shown that in several types of E. gracilaris light grown and dark grown cells, a linear correlation

exists between the amount of chlorophyll synthesized and the variation in Do for colony forming ability. Since chlorophyll per se is a relatively poor UV absorber (see review: 96) other substances related to the photosynthetic apparatus were believed by Hill *et al* to serve as a UV filter, thereby accounting for their 6 fold variation in Do values between light and dark grown cells. As an example of three of these substances, Brawerman *et al* (see review: 95) have shown that the RNA and protein content increases by about 40% in dark grown cells induced to form chloroplasts and Stern *et al* (see review: 95) have shown that ergosterol, which has a large UV absorption cross-section, is present in larger amounts in light grown than dark grown cells. In *O. cardiacum* it is also possible that decreases in the relative amounts of unknown substances in winter grown cells and hence decreased shielding of the nucleus could explain the 2 fold difference in radiosensitivity.

The seasonal difference in radiosensitivity could also be interpretated by assuming a difference in the efficiency of the repair mechanisms for winter and summer grown cells. No evidence has been found in the literature for any other work that might substantiate this hypothesis. In addition, a preliminary investigation on photoreactivation suggests that UV-irradiated cells from either period are equally photoreactivable.

As described earlier, a persistent second shoulder at about 10% was found on the survival curves at all cell ages. The second component of the curve was initially believed to represent a UV-resistant mutant. However, since as shown in Fig. 12, the radiosensitivity of the progeny from single cells which had survived a high dose of UV radiation was comparable to the radiosensitivity of the cells from "normal" cultures, the apparent resistance of cells in the second component of the survival curve was not inheritable.

Several experimenters, for example Elkind and Sutton (74) with S. cerevisiae, Deering (61) with B. emersonii and Horsley et al with O. cardiacum (78) have also obtained complex survival curves exhibiting a second shoulder following ionizing radiation. Both Elkind and Sutton and Deering have obtained similarly shaped complex curves using UV radiation. The explanation offered by these investigators to explain the shape of the curves is based on the presence of a small moiety of cells whose existence is attributed to either the decay in synchrony of the cell population or, in the case of Elkind and Sutton to a mixed population of divisional and interdivisional cells. These small moieties have survival parameters, Do and n, significantly different from those of the main group of cells and the final survival curve of the population is explained by the addition of the survival curves of the two moieties mixed in proportion to the relative size of

the two moieties. For example, with O. cardiacum the complex survival curve following ionizing radiation is obtained only for cells irradiated in G_2. At the middle of G_2, the population consists of approximately 70% G_2 cells and 30% S cells (82). Cells from these two stages differ in radiosensitivity by about a factor of 7 for their Do values and by a factor of about 40 for their n values. Such large changes in the parameters account for the presence of the second shoulder and subsequent decline in survival. Furthermore, as one would expect, for survival curves measured during G_2 the extrapolation of the second shoulder to the zero-ordinate axis varies depending on the proportion of S cells present in the predominantly G_2 population.

In contrast to these findings for ionizing radiation, with UV radiation in O. cardiacum the second shoulder is seen at all cell ages and furthermore the extrapolation of the second shoulder to the zero-ordinate axis is relatively constant (8 to 12%). In addition the n values of the initial portions of the survival curves at all cell ages are practically constant and the Do values change only by a factor of about 2.5. These points of difference make it difficult to explain the second shoulder in a similar way as was done with ionizing radiation.

Evidence has already been presented that appreciable cytoplasmic absorption does occur in O. cardiacum cells. As shown in Table A, Appendix D, there

is an appreciable variation in the position of the nucleus within the cell at each cell age. In Fig. 15, Appendix E a histogram of the measurements at 3 cell ages, 3 (G_1), 6 (S) and 13 (G_2) hr respectively are presented. At each cell age the histogram shows an atypical distribution of the measurement of the amount of intervening cytoplasmic material in front of the nucleus. Nuclei in those cells which are more remote from the apical cell wall (in the range 48 to 63 μ) would receive much less radiation than those nuclei which are closer to the apical wall. It is conceivable that these more remotely placed nuclei would receive little if any UV radiation at low or moderate dose levels. Hence, these cells would appear radioresistant in the population. Only when a high dose of UV radiation was employed would sufficient energy penetrate the intervening cytoplasm to inactivate the nucleus. Due to the limited knowledge about UV attenuation in these cells it is difficult to estimate from the histogram exactly what fraction of the cells would constitute this apparent radioresistant group. It is conceivable though, from an examination of the right hand side of the distribution, that it could be in the order of 10%.

The effect of this small group of cells with their nuclei situated more distal from the UV source could explain the initiation of the second shoulder. For example, with reference to Fig. 8 the appearance of the second shoulder occurs at about 17 K ergs/mm^2. At doses higher

than this (17 to 30 K ergs/mm^2) the 8% moiety not yet inactivated in the population would receive a dose to their nuclei less than you would expect by an amount proportional to the average percentage absorption of the extra intervening cytoplasmic material. If this were the only phenomenon present, the survival curve would not be expected to turn down as was observed experimentally. In order to explain this second turning down of the survival curve an additional mode of injury must be postulated which is only evident at relatively high doses (beyond 30 K ergs/mm^2). This additional mode of injury could very well be cytoplasmic in nature.

Support for UV cytoplasmic damage is seen in the work of Von Borstel and Wolff (35) who have shown dose-hatchability curves for UV-irradiated H. juglandis eggs. In their experiments they were able to shield the nucleus from UV radiation and hence obtain separate response curves for both nuclear and cytoplasmic damage. These response curves are shown in Appendix F. For nuclear UV damage the initial part of the curve showed little or no shoulder region; however, for only cytoplasmic damage the response curve showed a relatively large shoulder before an exponential decline in response. In the nuclear response curve they observed the initiation of a second shoulder at approximately the 33% survival level which they attributed to cytoplasmic absorption. Unfortunately they did not carry this response curve to dose levels beyond the end of

the shoulder region in the cytoplasmic damage response curve. Therefore they did not observe a second exponential decline. It would seem reasonable in reviewing their work to expect that they would have observed this phenomenon if they had gone to higher dose levels when irradiating the nucleus.

Swann (68) has suggested that the break on the survival curves of S. pombe could be due to the existence of a fairly clearly defined threshold for damage of a physiological sort. He observed at high doses that his cells died sooner and often without completing a single post-irradiation division. He suggested that at these doses non-genetic damage was superimposed on genetic damage. In contrast, in O. cardiacum it is suggest that cytoplasmic damage is superimposed on genetic damage only at very high dose levels and that this accounts for the second decline in survival.

Cytoplasmic damage, involving the photosynthetic machinery has been reported by several investigators (see review: 96). Van Baalen (97) has observed that in the blue-green alga Agmenellum quadruplicatum, a major part of the UV-induced damage up to a dose of 7350 ergs/ mm^2 occurred in some part of the photosynthetic machinery. The same dosages that caused decreased survival also killed photosynthesis, and the same photoreactivation conditions required to bring the survival level back to 100% also resulted in the complete recovery of photosynthesis. From these results he concluded that the

chromophores for UV damage and the action of photo-reactivation were in the photosynthetic machinery and did not involve DNA. In similar experiments with Chlorella pyrenoidosa he found that at approximately twice the UV dose for A. quadruplicatum, photosynthesis decayed with similar kinetics. In contrast to A. quadruplicatum, the decay was not photoreactivable. Bell and Merinova (see review: 96) measured photosynthetic inhibition in C. pyrenoidosa and concluded that the inhibitory effect was produced by the interaction of UV radiation and nucleic acids contained within the chloroplast. Halldal (96) has shown that in the green alga Ulva lactuca, photosynthetic inhibition is at a maximum at 220 mu. At 260 mu, the relative efficiency of inhibition was less than 25%. He believed that photosynthetic inhibition was due to protein and enzyme inactivation since at wave-lengths where DNA abosrbed insignificantly (223 to 238 mu) inhibition was reversible. It is possible that cytoplasmic damage to the chloroplast and subsequent photosynthetic inhibition may also be correlated with loss of reproductive ability in UV-irradiated O. cardiacum. However, since considerable evidence has been presented that the major effects of UV radiation are primarily at the nuclear level (see Introduction) and since Marcenko (34) has shown that in the green algae Netrium digitus reversal of UV-induced damage of reproductive ability is mainly associated with the nucleus, it is believed that in O. cardiacum loss of

reproductive ability following 254 mu irradiation is primarily (90%) associated with nuclear damage.

Another possible explanation for the second shoulder can be made which postulates the presence of a small but constant moiety of cells at all ages which are physiologically different from the main group. Cells in this group are presumed to have a highly efficient repair mechanism which does not become saturated until relatively high dose levels. When it does become saturated it could explain the presence of the second shoulder and subsequent decline in survival. Zamenhof and Reddy (93) have suggested this hypothesis to account for the plateau or plateau followed by an increase in mutation frequency at low survival levels of UV-irradiated B. subtilis spores. They believed that the efficiency of the mechanism that repaired UV-induced mutagenic lesions was different at different levels of survival.

The age-dependent response for UV radiosensitivity of Oedogonium cells is similar in shape to the response observed by Horsley and Pujara (79) for O. cardiacum cells exposed to ionizing radiation (Fig. 14). Cells were most resistant to both types of radiation during mid S and most sensitive during the latter part of G_2. The response to the two types of radiation differs in that n remains essentially constant for cells exposed to UV radiation but changes by a factor of 40 for

ionizing radiation. The kinetics of cellular division following the two types of radiation was observed to be quantitatively different. Up to 87% of the non-surviving progeny from UV-irradiated cells were unable to complete a single post-irradiation division. In contrast, with ionizing radiation about 90% of the non-survivors at all dose levels up to 16 K rads divided at least once (81). Djordjevic and Tolmach (47) have also observed that x-irradiated HeLa cells are able to enter, and usually to complete, mitosis following irradiation at dose levels leaving only a few percent of the cells viable. In contrast, a UV dose that left more than 1% of the cells viable gave evidence of destroying the majority of cells within 30 hours. Why destruction is slower with x-rays is not known.

A further difference observed qualitatively between the two radiations in O. cardiacum was seen with respect to the different expressions of radiation damage among the non-surviving progeny. For example, there were relatively very few giant cells seen in the non-surviving progeny at all cell stages. In contrast, for ionizing radiation up to 50% of the cells irradiated at 8 K rads produced filaments in which at least one of the cells was a giant (81). Rauth and Whitmore (67) and Lee and Puck (101) have pointed out that few giant cells are produced by UV radiation in mammalian cells in comparison to ionizing radiation.

The similarity in the stage dependent responses between UV and ionizing radiations suggests that the same target material is involved. However, the differences noted above suggest that the nature of the damage inflicted is different.

SUMMARY AND CONCLUSIONS

As was pointed out in the Preface the aim of this investigation was to determine the UV radiosensitivity of synchronously growing Oedogonium cardiacum cells. The radiosensitivity has been measured at different times during the first generation cycle and compared to the x-irradiation response. The variation in UV radiosensitivity was about 2.5 fold with cells in mid S stage being the most resistant and cells in late G_2 the most radiosensitive. It is believed that most of the variation in stage radiosensitivity can be attributed to differences in the efficiencies of the repair mechanisms at different cell ages. Evidence has also been presented to show that the magnitude of the UV radiosensitivity was different in the winter and summer months of the experimental period. This seasonal variation is explained by differences in cytoplasmic absorption of the UV beam.

The complex shape of the measured survival curves at all cell ages indicates the presence of a small group (10%) of cells exhibiting a marked difference in radiosensitivity. The existence of these inflection points on the survival curves is attributed to differences in the attenuation of the UV intensity in passing through the cell.

It was shown that variations exist between cells for the distance between the nucleus and the apical cell wall large enough to account for marked irregularities in the amount of irradiation received by the nucleus. Since it is postulated that the nucleus is primarily the target site for UV inactivation, the nucleus in the small group of cells would be additionally shielded by the increased amount of intervening cytoplasm. The effect of this shielding would introduce a break into the survival curve. The exponential decline following this break is attributed to cytoplasmic damage superimposed on nuclear damage at high dose levels. This explanation is favoured but other hypotheses have also been considered which at the present time can not be eliminated as possible explanations for the complex shape of the curve.

The similarities between the UV and X-ray age dependent response suggest that the targets principally damaged by both radiations are the same while the kinetics of cell growth following irradiation and the different expressions of radiation damage suggest that the mechanisms of action of the two radiations are fundamentally different.

A number of hypotheses have been suggested to explain the shape of the complex survival curves and the variations in sensitivity at each cell stage. Further experiments are planned with Oedogonium cardiacum to test the validity of some of these hypotheses.

(1) Further studies on photoreactivation at different light intensities to determine what amount

of visible light is necessary to bring about maximum photoreactivation and if photoreactivation is stage dependent.

(2) Measurements of chlorophyll content in summer and winter grown cells to determine if seasonal sensitivity variations are attributable to differences in the cellular components associated with photosynthesis.

(3) Microspectrophotometric studies on UV absorption through different parts of the cell using a microbeam of 254 mu radiation.

(4) Studies on the radiosensitivity of progeny from successive subcultures of UV-irradiated single cells to determine if a UV resistant strain can be isolated.

(5) A quantitative measurement of different morphological expressions of UV radiation damage observed throughout the experiments.

(6) Experiments on split dose studies (Elkind effect) to search for recovery from UV radiation sub-lethal damage. Results in the literature are contradictory regarding the presence of this phenomenon.

APPENDIX

APPENDIX A

SOIL EXTRACT - after Horsley and Fucikovsky (76)

Combine 50 ml of dry powdered soil with 600 ml of distilled water, boil for 2, 2 hour periods of 1 week interval and then decant. Filter supernatant through qualitative and glass fiber filter paper (3x) and dilute with distilled water to concentration required.

MODIFIED MACHLIS' OEDOGONIUM MEDIUM E (98)

$CaCl_2$	0.069g
KH_2PO_4	0.200
KNO_3	2.020
$MgSO_4 \cdot 7H_2O$	0.250
K_2HPO_4	0.090

Dissolve in 1,000 ml distilled water, add 1 ml trace element solution and 1 ml vitamin B_{12}.

Final pH = ca. 6.5

TRACE ELEMENT SOLUTION - after Hutner et al (99)

H_3BO_3	1.00g
$CuSO_4 \cdot 5H_2O$	0.15
EDTA (Na)	5.00
$ZnSO_4 \cdot 7H_2O$	2.20
$CaCl_2$	0.62

$MnCl_2 \cdot 4H_2O$	0.50g
$FeSO_4 \cdot 7H_2O$	0.50
$CaCl_2 \cdot 6H_2O$	0.12
$(NH_4)_6 \cdot Mo_7O_{24} \cdot 4H_2O$	0.10

Add to 75.0 ml distilled water, boil and cool slightly. Adjust pH to ca. 6.5 by the addition of solid KOH pellets and dilute final solution to 100 ml by the addition of distilled water.

APPENDIX B

FEULGEN STAINING TECHNIQUE

(Emmel and Cowdry (100))

FIXING: Remove slides from culture vessels, spray with distilled water and fix in filtered Carnoy's solution saturated with $FeNH_4 (SO_4) .12H_2O$ for 15 minutes. Rinse each slide in 95% EtOH for 5 minutes and then dip in dilute collodion (10 ml ether, 80 ml absolute ether, 10 ml collodion) for 2 minutes. This prevents loss of cells from the slide during the staining procedure. Place slides in ethanol chloroform for 5 minutes to harden the collodion.

Pass slides through the following series:

STAINING: 50% EtOH - 5 min
running tap water - 10 min
60°C 1N HCl - 13 to 17 min
Feulgen - 1 hr
SO_2 water - 13 min
running tap water - 15 min

DEHYDRATION: 50% EtOH - 3 min

70% EtOH - 3 min

80% EtOH - 3 min

95% EtOH - 3 min

100% EtOH - 3 min

100% EtOH and ether (9:1) - 2 to 5 min until collodion is removed

100% EtOH - 2 min

100% EtOH and xylol - 1 min

xylol - 30 min

Mount each slide with diluted permount (2 parts xylol and 1 part permount).

FEULGEN'S REAGENT

Dissolve 2g Basic Fuschin in 400 ml distilled boiling water, cool to 50°C and add 40 ml 1N HCl. Cool to 25°C and add 2g $Na_2S_2O_5$. Refrigerate overnight and add 4g Norit, filter and store in dark bottle.

SO_2 WATER

Dissolve 1.5g $NaHSO_3$ in 30 ml distilled water. Add 25 ml 1N HCl and dilute to 500 ml by the addition of distilled water.

APPENDIX C

ϕX-174 BACTERIOPHAGE AS A BIOLOGICAL DOSIMETER

Dilute ox-174 phage in PBS to approximately 10^6 pfu/ml and irradiate in an open petri dish. Remove small aliquots at regular intervals and dilute in PBS. Determine pfa of irradiated phage by soft agar technique. Combine 0.2 ml phage, 0.2 ml E. coli C and 3 ml soft agar. Pour over agar plates and incubate for 3 to 6 hr at 37°C. Count each plate for number of plaques and determine the survival curve for pfa of the bacteriophage assuming single hit target kinetics and a Do of 85 ergs/mm^2. Apply correction factor of Morowitz (91) for UV absorption by medium, to determine the incident intensity on the surface of the medium.

PBS SOLUTION: NaCl 8.00g Na_2HPO_4 1.15g
KCl 0.20 KH_2PO_4 0.20

Dissolve in 1 litre of distilled water and sterilize by millipore filtration.

AGAR:	Soft agar	Bottom agar
	8g Special Noble agar(i)	10g Special Noble agar
	8g nutrient broth(i)	8g nutrient broth
	1 litre distilled water	1 litre distilled water

(i) Fisher (Difco) Laboratories, Toronto, Ontario.

Autoclave to sterilize. Keep soft agar at 42°C. Pour ca. 10 ml of bottom agar into 100 x 15 mm petri dishes and cool.

E. COLI C

Prepare overnight cultures in Bacto nutrient broth. Grow at 37°C to a concentration of approximately 10^8 cells/ml.

APPENDIX D

TABLE A

Cell Measurements for Different Ages in the First Generation Cycle of Feulgen Stained Cells

Cell Age (hr)	Cell Dimensions (u)	Nucleus Dimensions (u)	Distance (u) Between the Apical Cell Wall and Nuclear Membrane	Center of Nucleus		
(1)	(2)	(3)	(4)	(5) *		
1.8	96.6 x 30.4	10.5 x 7.2	37.2 ± 4.6	42.4	42.1	G_1
3.0	97.8 x 30.3	13.0 x 7.0	35.3 ± 7.1	41.8		
5.0	101.1 x 29.8	9.6 x 8.0	33.2 ± 6.3	38.0	40.7	S
6.0	99.3 x 30.0	8.9 x 9.4	35.9 ± 7.1	40.4		
7.5	94.1 x 29.6	11.2 x 11.7	37.0 ± 8.5	42.6		
8.8	104.5 x 29.8	9.5 x 7.2	37.0 ± 6.8	41.7		
11.0	97.9 x 27.3	11.5 x 9.3	35.3 ± 6.3	41.0	40	G_2
13.0	102.8 x 31.3	13.0 x 11.7	32.5 ± 7.7	39.0		
15.0	106.0 x 30.4	14.6 x 12.4	30.5 ± 7.3	37.8	late M	G_2

* The values in column (5) have been determined by the addition of one-half column (3) plus column (4).

APPENDIX E

FIG. 15

Comparison of the histograms of the distance between the outer nuclear membrane and apical cell wall for cells age 3(G_1), 6(S), and 13(G_2) hr respectively.

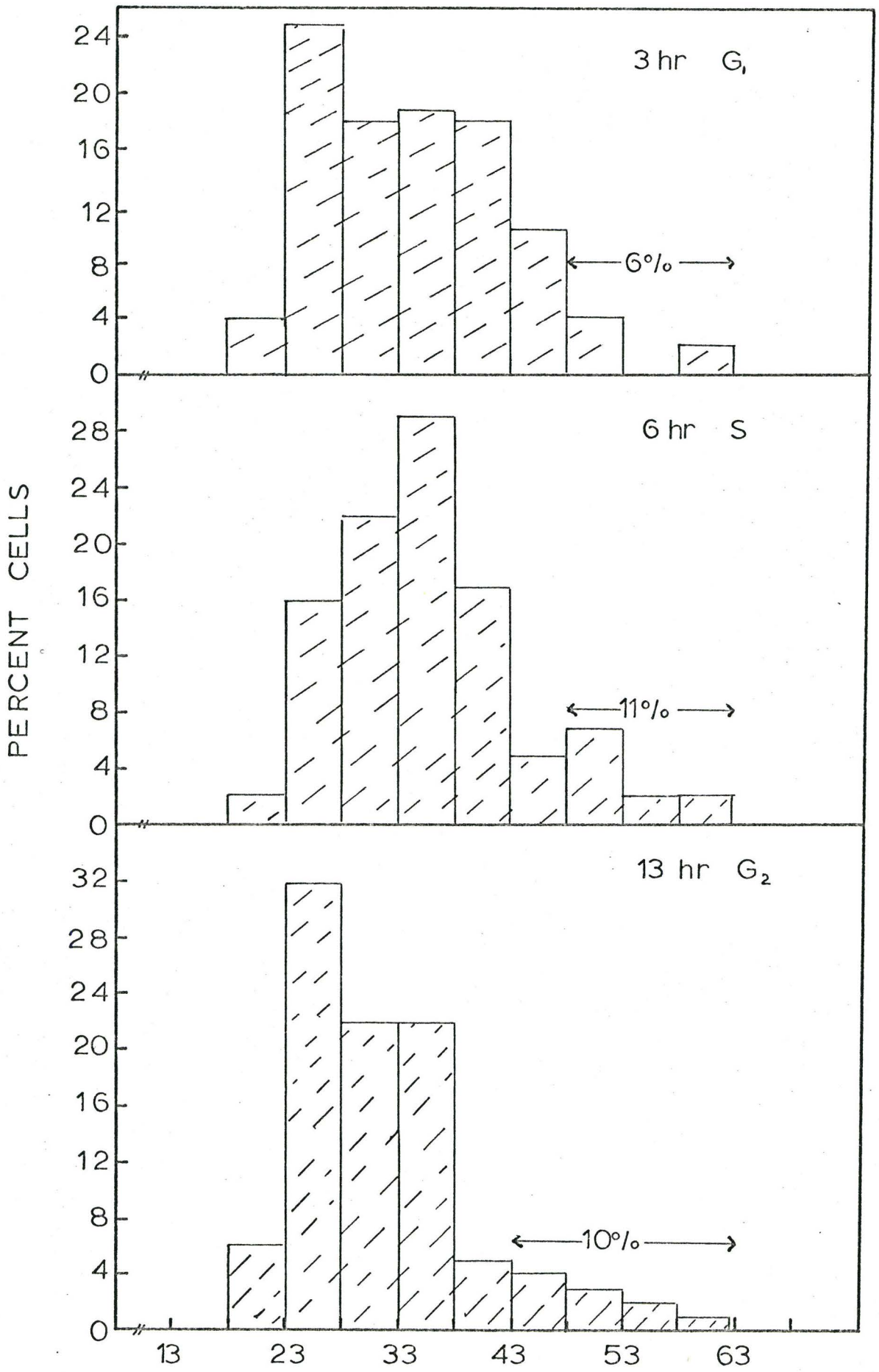
3 hr G1
6%
6 hr S
11%
13 hr G2
10%
PERCENT CELLS
0
4
8
12
16
20
24
28
32
13
23
33
43
53
63
DISTANCE BETWEEN APICAL CELL WALL
AND OUTER NUCLEAR MEMBRANE - μ

APPENDIX F

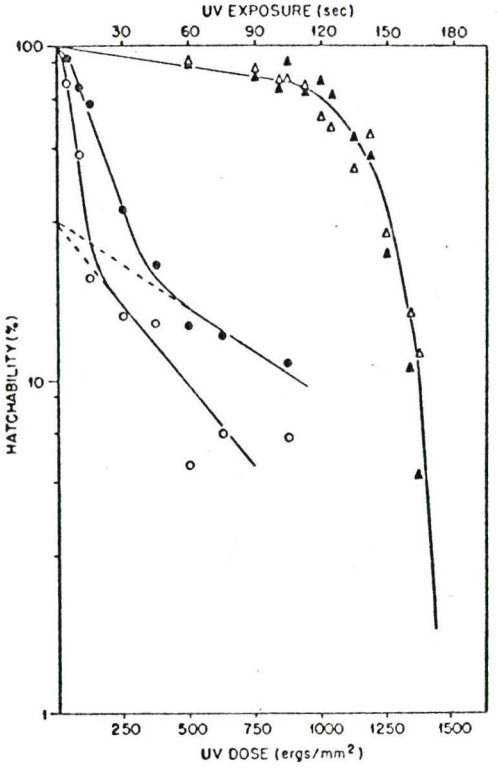

FIG. 3.—Dose-hatchability curves for *Habrobracon* eggs irradiated on their convex (nuclear) (○, ultraviolet; ●, ultraviolet plus photoreactivating light) or concave (nonnuclear) (△, ultraviolet; ▲, ultraviolet plus photoreactivating light) surfaces.

BIBLIOGRAPHY

1. J.K. Setlow in Current Topics in Radiation Research Vol. II, Ebert and Howard, North-Amsterdam, 1963.

2. A.G. Giese, Physiol. Rev. 30, 431 (1950).

3. J. Jagger, Introduction to Research in Ultraviolet Photobiology, Prentice-Hall, Inc., N.J., 1967.

4. A. Hollaender, (ed), Radiation Biology Vol. II, Ultraviolet and Related Radiations, McGraw Hill Book Co., Inc., N.Y., 1955.

5. E.J. Bowen, (ed), Recent Progress in Photobiology, Blackwell Scientific Pub., Oxford, 1965.

6. G.W. Rushizky, M. Riley and L.S. Prestidge, Biochem. et Biophys. Acta 45, 70 (1960).

7. J.K. Setlow, Photochem. Photobiol. 3, 405 (1962).

8. R. Beukers and W. Berends, Biochem. et Biophys. Acta 49, 181 (1961).

9. R.A. Deering, Sci. Amer. 207, No. 6, 135 (1962).

10. D.O. Rahn, R.G. Shulman and J.W. Longworth, Rad. Res., Suppl. 7, 139 (1967).

11. A.Y. Varghese and S.Y. Wang, Science 160, 186 (1968).

12. H.E. Johns, M.L. Pearson, J.C. LeBlanc and C.W. Helleiner, J. Mol. Biol. 9, 503 (1964).

13. P. Alexander and H. Moroson, Nature 194, 882 (1962).

14. R.B. Setlow and J.K. Setlow, Proc. Natl. Acad. Sci. U.S. 48, 1250 (1962).

15. J.E. Trosko, E.H. Chu and W.L. Carrier, Rad. Res. 24, 667 (1965).

16. D.L. Wulff, J. Mol. Biol. 7, 431 (1963).

17. J.K. Setlow and M.E. Boiling, Biochem. Biophys. Acta, 108, 259 (1965).

18. C.W. Helleiner, M.L. Pearson and H.E. Johns, Proc. Natl. Acad. Sci. U.S. 50, 761 (1963).

19. P.A. Swenson and R.B. Setlow, Photochem. Photobiol. 2, 419 (1963).

20. L. Grossman, Proc. Natl. Acad. Sci. U.S. 48, 1609 (1962).

21. K.C. Smith, Biochem. Biophys. Res. Comm. 8, 157 (1962).

22. A.D. McLaren and D. Shugar, Photochemistry of Proteins and Nucleic Acids, Pergamon Press, Long Is. City, N.Y., 1964.

23. R.E. Rasmussen and R.B. Painter, Nature 203, 1360 (1964).

24. W. Harm, Mutation Res. 6, 25 (1968).

25. A.M. Rauth, Rad. Res. 31, 121 (1967).

26. D.R. Davies, Mutation Res. 2, 477 (1965).

27. J.K. Setlow, Rad. Res., Suppl. 6, 141 (1966).

28. P. Howard-Flanders and R.P. Boyce, Rad. Res. (Suppl. 6), 156 (1966).

29. C.S. Rupert, J. Gen. Physiol. 45, 703 (1962).

30. C.S. Rupert, J. Gen. Physiol. 45, 725 (1962).

31. D.L. Wulff and C.S. Rupert, Biochem. Biophys. Res. Comm. 7, 237 (1962).

32. H. Werbin and C.S. Rupert, Photochem. Photobiol. 7, 225 (1968).

33. J.K. Setlow, Photochem. Photobiol. 3, 405 (1964).

34. E. Marcenko, Rad. Bot. 8, 325 (1968).

35. R.C. von Borstel and S. Wolff, Proc. Natl. Acad. Sci. U.S. 41, 1004 (1955).

36. A.G. Giese, Proc. Intern. Congr. Photobiol. 3rd., Copenhagen, Elsevier, Amsterdam 1960.

37. C.L. Brandt and A.C. Giese, J. Gen. Physiol. 39, 735 (1956).

38. R.B. Setlow and W.L. Carrier, Proc. Natl. Acad. Sci. U.S. 51, 226 (1964).

39. C.E. Terry and J.K. Setlow, Photochem. Photobiol. 6, 799 (1967).

40. J.H. Wu, R.A. Lewin and H. Werbin, Virology 31, 657 (1967).

41. R.P. Boyce and P. Howard-Flanders, Proc. Natl. Acad. Sci. U.S. 51, 293 (1964).

42. R. Latarjet, C.R. Acad. Sci. 217, 186 (1943).

43. P. Van de Putte, C.A. van Sluis, J. van Dillewijn and A. Rorsch, Mut. Res. 2, 97 (1965).

44. P. Howard-Flanders and R.P. Boyce, Genetics 50, 256 (1964).

45. W. Szybalski, Rad. Res. (Suppl. 7), 147 (1967).

46. W.K. Sinclair and R.A. Morton, Biophys. J. 5, 1 (1965).

47. B. Djordjevic and L.J. Tolmach, Rad. Res. 32, 327 (1967).

48. Y. Skreb and M. Errera, Exptl. Cell Res. 12, 649 (1957).

49. R.F. Kimball, In: Advances in Radiation Biology, Vol. 2, Augenstein, Mason and Zelle, Academic Press, N.Y., 1965.

50. B.D. Howard and I. Tessman, J. Mol. Biol. 9, 372 (1964).

51. L. Haas and C.O. Doudney, Nature 185, 637 (1960).

52. H.D. Kumar, Ann. of Bot. N.S. 27, 723 (1963).

53. R.A. Lewin, J. Gen. Microbiol. 6, 233 (1952).

54. M.B. Allen and S. Bendix, Arch. Mikrobiol. 42, 36 (1962).

55. I.D. Anivkeeva, E.N. Vaulina and V.A. Shevehenko, Radiobiologiya 4, 883 (1964).

56. R.H. Humphrey, W.C. Dewey and A. Cork, Rad. Res. 19, 247 (1963).

57. A.C. Faberge, Genetics 36, 549 (1951).

58. A. Howard and S.R. Pelc, Hered., Suppl. 6, 261 (1953).

59. L.G. Laytha, R. Oliver and F. Ellis, Brit. J. Cancer 8, 367 (1954).

60. M. Domon and A.M. Rauth, Rad. Res. 35, 350 (1968).

61. R.A. Deering, Rad. Res. 34, 87 (1968).

62. J.E. Cleaver, Biochem. et Biophys. Acta 108, 42 (1965).

63. J.E. Cleaver, Rad. Res. 30, 795 (1967).

64. P.P. Dendy and J.E. Cleaver, Int. J. Rad. Biol. 8, 301 (1964).

65. J.F. Scaife and H. Brohee, Int. J. Rad. Biol. 13, 531 (1968).

66. C.H. Hood, Mut. Res. 6, 391 (1968).

67. A.M. Rauth and G.F. Whitmore, Rad. Res. 28, 84 (1966).

68. M.M. Swann, Nature 193, 1222 (1962).

69. J.E. Cleaver, Nature 209, 1317 (1966).

70. D.L. Steward and R.M. Humphrey, Nature 212, 298 (1966).

71. A.R. Hipkiss, Rad. Bot. 7, 347 (1967).

72. L.J. Stadler and F.M. Uber, Genetics 27, 84 (1942).

73. C. Helmstetter and R.B. Uretz, Biophys. J. 3, 35 (1963).

74. M.M. Elkind and H. Sutton, Rad. Res. 10, 283 (1959).

75. R.L. Erikson and W. Szybalski, Rad. Res. 18, 200 (1963).

76. R.J. Horsley and L.A. Fucikovsky, Int. J. Rad. Biol. 4, 409 (1962).

77. R.J. Horsley and L.A. Fucikovsky, Int. J. Rad. Biol. 5, 417 (1963).

78. R.J. Horsley, L.A. Fucikovsky and S.N. Banerjee, Rad. Bot. 7, 241 (1967).

79. R.J. Horsley and C.M. Pujara, Rad. Res. In the press (1969).

80. M. Banerjee, S.N. Banerjee and R.J. Horsley, Int. J. Rad. Biol. 2, 395 (1966).

81. R.J. Horsley, S.N. Banerjee and M. Banerjee, Rad. Bot. 7, 465 (1967).

82. S.N. Banerjee and R.J. Horsley, Exptl. Cell Res. 53, 549 (1968).

83. L.R. Hoffman, Ph.D. Thesis, The University of Texas, 1961.

84. F.E. Fritsch, The Structure and Reproduction of the Algae, Cambridge University Press, 1965.

85. R.A. Lewin, (ed), Physiology and Biochemistry of Algae, Academic Press, N.Y., 1962.

86. C.T. Retallack and K.C. von Maltzahn, Can. J. Bot. 46, 767 (1968).

87. V.W. Burns, Progr. Biophysics and Biophysic Chem. 12, 1 (1962).

88. S.N. Banergee and R.J. Horsley, Amer. J. Bot. 55, 514 (1968).

89. J.C. Davis and R.L. Sinsheimer, J. Mol. Biol. 6, 203 (1963).

90. H.J. Morowitz, Science 111, 224 (1950).

91. J. Lenoble and B. St. Guilly, C.R. Acad. Sce. 240, 955 (1955).

92. A.M. Rauth, Biophysics J. 5, 257 (1965)

93. S. Zamenhof and T.K. Reddy, Rad. Res. 31, 112 (1967).

94. A.S. Pietro, Harvesting the Sun, Acad. Press, N.Y., 1967.

95. H.Z. Hill, J.A. Schiff and H.T. Epstein, Biophysic. J. 6, 125 (1966).

96. Per Halldal, Photochem, Photobiol. 6, 445 (1967).

97. C. van Baalen, Plant Phys. 43, 1689 (1968).

98. L. Machlis, A.J. Bot. 49, 171 (1962).

99. J.R. Stein, A. J. Bot. 45, 664 (1958).

100. V.M. Emmel and E.C. Cowdry, Laboratory Technique in Biology and Medicine, Williams and Wilkins Co., Baltimore, 1964.

101. H.H. Lee and T.T. Puck, Rad. Res. 12, 340-348 (1960).

102. M.M. Elkind and G.F. Whitmore, The Radiobiology of Cultured Mammalian Cells, Gordon and Breach, N.Y., 1967.

103. W.K. Sinclair, Rad. Res. 33, 620 (1968).

104. S.S. Wilks, Elementary Statistical Analysis, Princeton University Press, U.S.A., 1956.